DIRECT INITIATION THROUGH DETONATION BRANCHING IN A PULSED DETONATION ENGINE

THESIS

Alexander R. Hausman
Second Lieutenant, USAF

AFIT/GAE/ENY/08-M17

DEPARTMENT OF THE AIR FORCE
AIR UNIVERSITY

AIR FORCE INSTITUTE OF TECHNOLOGY

Wright-Patterson Air Force Base, Ohio

The views expressed in this thesis are those of the author and do not reflect the official policy or position of the United States Air Force, Department of Defense, or the United States Government.

AFIT/GAE/ENY/08-M17

DIRECT INITIATION THROUGH DETONATION BRANCHING IN A PULSED DETONATION ENGINE

THESIS

Presented to the Faculty

Department of Aeronautical and Astronautical Engineering

Graduate School of Engineering and Management

Air Force Institute of Technology

Air University

Air Education and Training Command

In Partial Fulfillment of the Requirements for the

Degree of Master of Science in Aeronautical Engineering

Alexander R. Hausman, B.S.M.E.

Second Lieutenant, USAF

March 2008

AFIT/GAE/ENY/08-M17

DIRECT INITIATION THROUGH DETONATION BRANCHING IN A PULSED DETONATION ENGINE

Alexander R. Hausman, B.S.M.E.
Second Lieutenant, USAF

Approved:

//SIGNED//	12 March 2008
Paul I. King, PhD (Chairman)	Date
//SIGNED//	12 March 2008
Maj Richard D. Branam, PhD (Member)	Date
//SIGNED//	12 March 2008
Mark F. Reeder, PhD (Member)	Date

Abstract

Pulsed Detonation Engines are currently limited in operating frequency to the order of 40 Hz due to lengthy ignition and deflagration to detonation transition (DDT) times. An experimental study is conducted to determine the requirements necessary to eliminate these constraints through the concept of direct initiation. A branched detonation crossover setup is constructed and the operational requirements are determined.

This research demonstrates the ability to directly initiate a detonation in a vacant tube from a detonation obtained through detonation branching. Using a hydrogen-air mixture, a tail-to-head detonation branching is achieved in which a detonation is seen to propagate from a spark ignited detonation tube, through a crossover tube and across a 1:2 diameter expansion ratio into a vacant second detonation tube. This effectively eliminates the ignition and DDT times associated with the conventional operation of the second tube. The closed-end pressure trace of a transferred detonation as deemed successful through wave speed measurements is analyzed and further solidifies the findings.

Acknowledgments

I would first like to extend thanks to my advisor, Dr. Paul King for the opportunity to perform research away from the computer labs and in a hands-on atmosphere. I greatly appreciate the time, support and guidance you have provided throughout this incredible learning opportunity. Also at AFIT, I thank my committee members, Dr. Mark Reeder and Maj Richard Branam for aiding in refining my work.

I must also thank everyone at the AFRL/RZTC Pulsed Detonation Research Facility (PDRF) for their never-ending support and time spent bringing me up to speed. Special thanks go to Dr. Fred Schauer and Dr. John Hoke for their continual flow of knowledge and technical support. I gratefully acknowledge the contribution of Curtis Rice for his assistance in enabling the research conducted and presented here. The day to day operations of the PDRF could not happen without his unfailing dedication. The learning curve associated with my research was greatly overcome due to the guidance and direction of Maj Dave Hopper. Thank you for the vast amounts of one-on-one guidance you provided during our time together.

To my family and friends, thank you for your support during my stay here at AFIT. The outlet you provided was much needed and appreciated. I would most certainly not be the man I am today without the input from each and every one of you. Most importantly, I give thanks to the Lord. As much as I no longer wanted to be in an education environment, I am very thankful and feel blessed to have been given this opportunity. Last, and by no means least, I'd like to thank God for blessing me with my fiancé, the love of my life, whom I met during my time at AFIT.

Table of Contents

List of Figures

Page

List of Tables

Page

List of Symbols

Acronyms

AFB – Air Force Base
AFIT – Air Force Institute of Technology
AFRL – Air Force Research Laboratory
RZTC – Propulsion Directorate, Turbine Engine Division, Combustion Science Branch
AIAA – American Institute of Aeronautics and Astronautics
CJ – Chapman-Jouguet
DDT – Deflagration to Detonation Transition
EF – Engine Frequency
FF – Fill Fraction
NPT – National Pipe Thread
MPT – Male National Pipe Thread
PDE – Pulsed Detonation Engine
PDRF – Pulsed Detonation Research Facility
PF – Purge Fraction
ZND – Zeldovich-von Neumann-Döring

Symbols

A – Arrhenius constant [1/s]
A – Cross-sectional area [cm^2]
a – Speed of sound [m/s]
C_p – Specific heat at constant pressure [J/kg*K]
d^* - Critical diameter [cm]
E_a – Activation energy [J]
$freq$ – Frequency [Hz]
h_f° – Heat of formation [J/mol]
MW – Molecular weight [kg/kmol]
$\dot{m}$ – Mass flow rate [kg/s]
n – Number of data points
p – Pressure [Pa or atm]
q – Heat of reaction [J/kg]
R – Specific gas constant [J/(kg*K)]
R_u – Universal gas constant [J/(kmol*K)]
T – Temperature [K]
t – Time [s]
u – Velocity [m/s]
V – Volume [L] [m^3]
x – Experimental mean
X_i – Uncertainty variable of interest
– Number of

Greek Symbols

γ – Ratio of specific heats
λ – Cell size [mm]
σ – Standard deviation
ϕ – Equivalence ratio
ρ – Density [kg/m^3]

DIRECT INITIATION THROUGH DETONATION

BRANCHING IN A PULSED DETONATION ENGINE

I. Introduction

Motivation

Interest in the field of Pulsed Detonation Engines (PDE) has increased greatly in recent years due in part to the potential for increased thermal efficiency derived from constant volume combustion as opposed to a constant pressure process as in turbine engines (Eidelman et al., 1991:1). In addition, PDEs are relatively inexpensive and the thrust produced has been previously shown to be scalable through the operating frequency and resulting cycle time (Schauer et al., 2001:1). The increase of the engine operating frequency through a reduction in cycle time directly relates to the thrust produced.

Pulse Detonation Engine Cycle

A PDE is an unsteady propulsion device that operates a series of single open-ended detonation tubes on a continuous fill-fire-purge cycle. A fuel-oxidizer mixture is injected into the tube and ignited from the closed end. Through the employment of Schelkin-like spirals or similar obstructions and an ignition source, the requirements for the formation of a detonation wave are met. The detonation is formed and through a constant volume process thrust is produced as it exits the tube. The thrust created is proportional to both the size of the detonation tube and the frequency of the detonations produced. The research presented here is conducted using a valved PDE consisting of three phases of equal time: fill, fire, and purge.

Fill Phase

During the fill phase, a fresh fuel-air mixture is allowed to enter into the detonation tube through the fill valves as shown in Figure 1. The ratio of the volume of the fuel-air mixture introduced to the volume of the detonation tube is referred to as the fill fraction (FF). Upon the closure of the fill valve, the fill phase is considered complete.

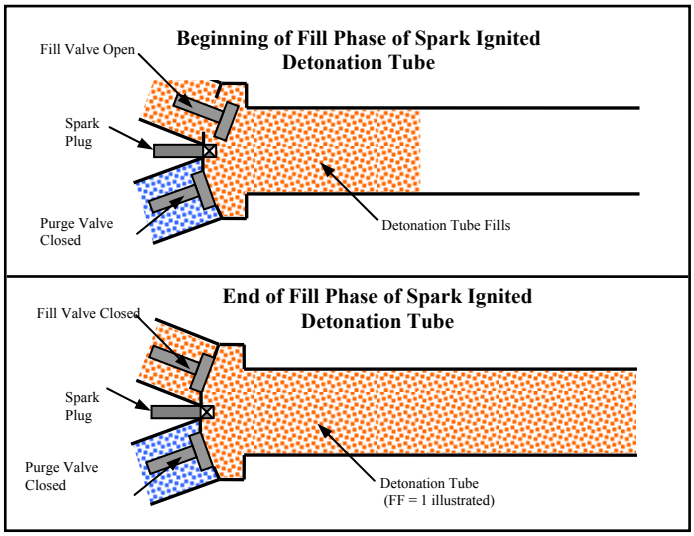

Figure 1. Schematic of the fill phase

Fire Phase

The fire phase is comprised of four different sub-phases: spark delay, ignition, detonation to deflagration transition (DDT), and blow down. The spark delay is a user specified pause between the closure of the fill valve and the spark deposit. The relevance in the current research is twofold: 1) to prevent backfires during research and 2) to allow the detonation created in the primary detonation tube to act as the ignition source for the second branch ignited detonation tube. The ignition time is defined as the time elapsed from spark deposit to the formation of combustion in the fuel-air mixture, which for low vapor pressure fuels is approximately 7-9 msec. The DDT time is that required for a

deflagration wave formed by the spark deposit to transition to a detonation wave as it travels downstream, as illustrated in Figure 2, and can be estimated to be approximately 2-2.5 msec. The detonation wave formation process will be discussed in greater detail later. The final sub-phase of the fire phase is known as blow down. This is the time required for the newly formed detonation wave to exit the detonation tube and an expansion wave to propagate back upstream to equilibrate pressure. This is the thrust producing phase of the PDE.

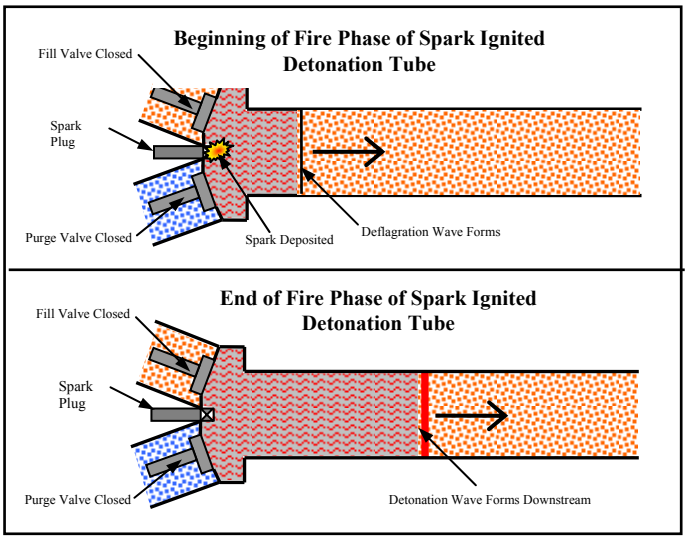

Figure 2. Schematic of the fire phase

Purge Phase

The purpose of the purge phase is to expel hot combustion products produced during the fire phase and to cool the tube walls in order to prevent auto-ignition of the next fuel-air mixture introduced. The purge phase begins when the purge valve opens and air enters the detonation tube as shown in Figure 3. Similar to the fill fraction, the ratio of the purge gas volume introduced during this phase to the tube volume is known as the purge fraction (PF).

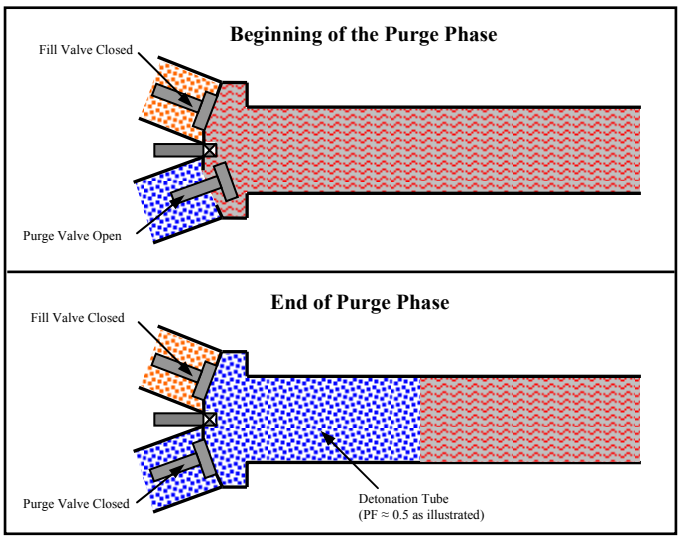

Figure 3. Schematic of purge phase

Problem Statement

For PDEs to produced adequate amounts of thrust and hence be a viable means of propulsion, they must be able to operate at high frequencies (Schauer et al., 2001). To obtain such higher frequencies, the individual cycle times must be reduced. Until recently the ignition time has proven to be a limiting factor in PDE operating frequencies. For example, a valved PDE using a long-chain hydrocarbon fuel has approximate fire sub-phase times as follows; 1) an ignition time of 7 msec, 2) a DDT time of 2 msec, and 3) a blow down time of 0.5 msec resulting in the total fire phase time of 9.5 msec. For a PDE consisting of three equal phases, the total time for one complete cycle would total 28.5 msec resulting in a corresponding maximum engine frequency of 35 Hz. Branch detonation has been shown to decrease ignition time and increase cycle performance in PDEs operating with hydrogen and n-heptane fuels (Tucker et al., 2003; Panzenhagen et al., 2004). The concept of detonation branching is that rather than igniting the detonation

with a relatively low-energy spark, a detonation from a neighboring source is used to ignite the fresh fuel-air mixture as illustrated in the idealized schematic of Figure 4.

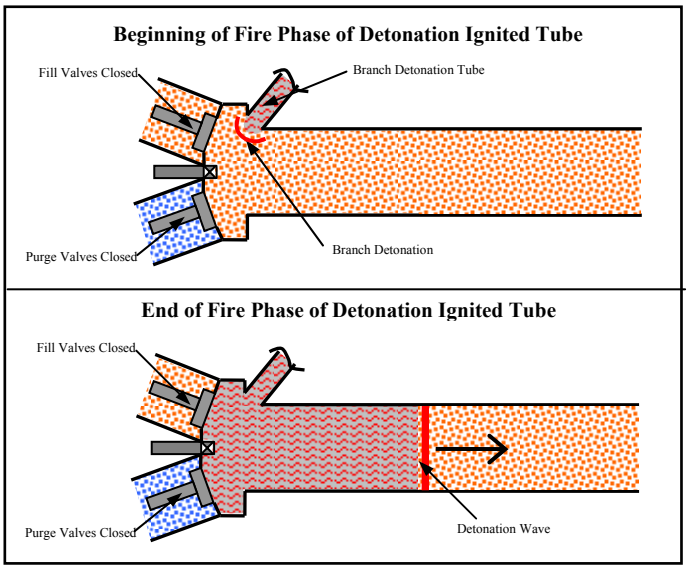

Figure 4. Schematic of branch detonation ignition

Upon introduction to the second detonation tube, a number of scenarios can be constructed by the branched detonation. On one extreme, the detonation can successfully mitigate the expansion into the second detonation tube and propagate downstream as a detonation. At the other end of the spectrum, the shock wave and combustion front can decouple at the expansion into the larger area and the combustion will continue downstream as a deflagration. With both cases, the ignition time is virtually eliminated and with the first case, the DDT time is also eliminated as the detonation is sustained throughout the transfer.

The intrinsic goal of all detonation branching research is to eventually serve as the foundation for the concept of a self-sustaining engine in which a detonation will continuously travel around the detonation tubes, igniting each successive tube at the correct time, as illustrated in Figure 5. The research presented here is a vital step towards the eventual implementation of this continuous PDE design.

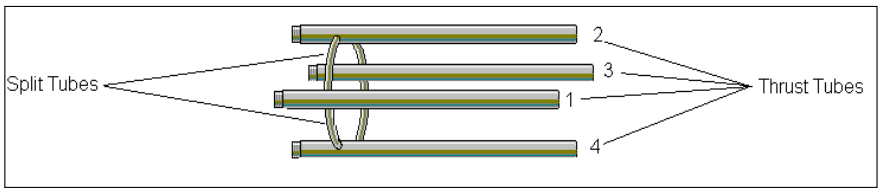

Figure 5. Concept of a self-sustaining continuously branched PDE

Various factors should be considered for the crossover tube as it is a non-thrust producing element. It should be sized to reduce thrust specific fuel consumption, ease the fabrication process and increase the practicality of use on future aircraft. These factors however, are vital to the eventual implementation of the crossover detonation branching setup on an aircraft and as such are not addressed to a great extent for the current research. Successful splitting of a detonation into a ¾ inch tube using hydrogen has been previously demonstrated (Rolling et al., 2002). Rolling verified the success of branching a detonation through an analysis of wave speeds. It was determined that successful detonation splitting can be obtained with numerous geometries and also that branch detonation can be harnessed to result in the strong ignition of a secondary detonation tube. Research performed by Panzenhagen was the first attempt at branch detonation with a flash vaporized liquid hydrocarbon fuel, n-heptane, and was conducted at a single equivalence ratio (Panzenhagen, 2004). Panzenhagen also recorded that ignition and DDT times were greatly reduced through the use of detonation branching. The research presented herein will further develop that presented initially by Rolling and Panzenhagen by utilizing the technique of detonation branching to directly initiate a second detonation tube. The eventual outcome will be determined through the analysis of wave speed measurements along all lengths of the experimental setup. The ignition and DDT times of a branch ignited detonation tube have both been extensively documented in prior research and as such will not be the focus of analysis herein.

Objectives and Procedure

The goal of this research was to construct an experimental setup and successfully demonstrate a direct initiation produced through detonation branching thereby providing a basis for a continuously branched PDE. The procedure required to meet said objective is as follows:

1. Design and construct a one inch crossover tube and branch detonation hardware.
2. Successfully perform detonation branching and deliver detonations to a second detonation tube.
3. Directly initiate a vacant second detonation tube using only the transferred detonation.
4. Analyze head pressure traces and wave speeds recorded in the second detonation tube to validate direct initiation.

Units

Unfortunately, the PDE community maintains little continuity pertaining to a unit system. Some authors use the international standard of units (S.I.), while others use the English system as a standard. As such, most dimensions here will be in the English system with the primary exception being wave speed measurements.

Organization

Chapter I served as a brief introduction to pulse detonation engine technology. In addition, the motivation, problem statement, and the goals for this work are discussed. Chapter II provides the theoretical background for this research starting with a discussion

on deflagration and detonation waves, pulse detonation engine theory, and the global reaction theory. Previous research and other information pertinent to the present research are then presented. In Chapter III, the facility, pulse detonation engine, instrumentation, test configurations, and methodology are discussed. Chapter IV is a summary of the results obtained from the data collected, complete with current pressure trace analyses compared to previous branched detonation data. Chapter V houses the all encompassing conclusions from the previous chapters and provides recommendations for further research.

II. Background and Theory

Ignition Time

In order for combustion to commence, the requirements for ignition of the fuel-air mixture in the tube must first be met. When the energy added to the constant volume system through spark deposition is greater than that of the activation energy, E_a, ignition will occur. Activation energy is simply the energy required to initiate the combustion reaction of a given fuel-oxidizer mixture; typically reported in units of J/mol. When this activation threshold is exceeded, the fuel reacts with the oxidizer to form highly reactive radicals. The number of radicals formed increases with the amount of fuel consumed, resulting in a localized explosion. The rapid release of energy consumes the reactants until a chemical equilibrium has been achieved. Chemical reactions obey what is commonly known as the Arrhenius Rate Law which relates the reaction temperature to the reaction rate. The corresponding ignition time is directly proportional to the reaction rate. As mentioned, ignition time is that elapsed from when the energy is deposited to the system to the point of ignition. The reaction rate is directly related to the temperature and pressure as stated below (Kuo, 2005:242):

$$IgnitionTime \propto \frac{1}{RR} = \frac{1}{A} p^{-n}[fuel]^{-m}[oxydizer]^{-j} e^{\left(\frac{E_a}{R_u T}\right)} \tag{1}$$

where *RR* is the reaction rate, A is the Arrhenius constant, p is the pressure, [fuel] is the fuel concentration, [oxidizer] is the oxidizer concentration, R_u is the universal gas constant, E_a is the activation energy, and T is the mixture temperature. The exponents n, m, and j are properties of the specific fuel analyzed. It is apparent from intuition and

verified by Equation (1) that raising the temperature or pressure results in a decreased ignition time.

Deflagration and Detonation Waves

There are two distinct modes of combustion that may be present during the operation of a pulsed detonation engine, deflagrations and detonations. A deflagration wave is a subsonic flame sustained by heat transfer produced through a chemical reaction. A detonation wave however, is a supersonic flame sustained by compression waves sent forth from a trailing reaction zone. The primary differences between deflagration and detonation waves are the wave speeds and pressure gradients. Table 1 summarizes the physical properties for deflagration and detonation waves, where subscripts one and two denote the conditions within the reactants and products region respectively as shown in Figure 6.

Table 1. Qualitative differences between detonation and deflagration properties (Kuo, 2005:357)

	Detonation	Deflagration
u_1/a_1	5 - 10	0.0001 - 0.03
u_2/u_1	0.4 - 0.7	4 - 6
P_2/P_1	13 - 55	~0.98
T_2/T_1	8 - 21	4 - 16
ρ_2/ρ_1	1.7 - 2.6	0.06 - 0.25

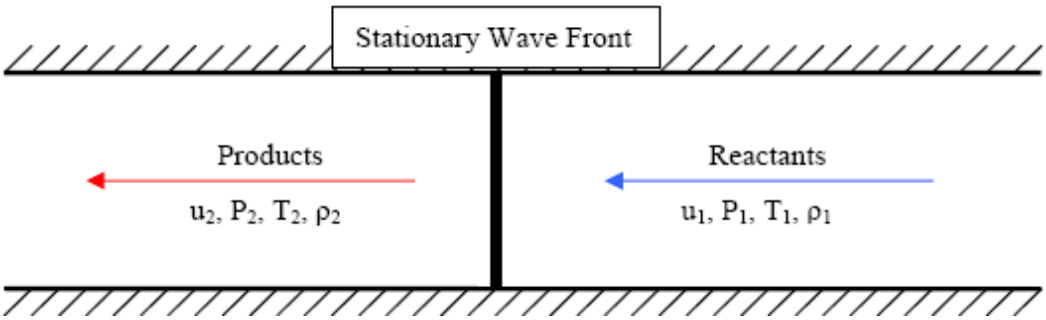

Figure 6. Schematic of stationary combustion wave

It is, among a number of items, the increase in density obtained through the presence of a detonation wave that provides the momentum change required to produce thrust for the PDE. A brief review of combustion wave theory is necessary to correctly understand the physical principles that govern detonation and deflagration flames.

Hugoniot Relations

The Hugoniot equation results in a plot containing all possible downstream solutions of density and pressure (ρ_2 and p_2 respectively) given the upstream values (ρ_1 and p_1) and the heat released per unit mass, q. The basis of this relation is derived from the conservation of mass, momentum, energy and the equation of state as shown in Equations (2), (3), (4), and (5) respectively:

$$\rho_1 u_1 = \rho_2 u_2 \tag{2}$$

$$p_1 + \rho_1 u_1^2 = p_2 + \rho_2 u_2^2 \tag{3}$$

$$C_p T_1 + \frac{u_1^2}{2} + q = C_p T_2 + \frac{u_2^2}{2} \tag{4}$$

$$p_2 = \rho_2 R_2 T_2 \tag{5}$$

where p is the pressure, ρ is the density, u is the velocity, C_p is the specific heat at a constant pressure, T is the temperature, q is the heat of combustion, and R is the universal gas constant. The equations assume one-dimensional flow, no body forces, no external heat addition, negligible species inter-diffusion effects, and no change in temperature or velocity over distance (Kuo, 2005:358). This type of representation allows the combustion event to be collapsed into a discontinuity; the combustion wave. The gas is assumed to be calorically perfect, and therefore both C_p and the ratio of specific heats, γ

are assumed to be constant. Well know definitions of C_p and γ are used to obtain the relationship:

$$C_p = \frac{\gamma}{\gamma - 1} R \tag{6}$$

Substituting Equations (6) and (5) into Equation (4), an updated expression for the conservation of energy is obtained (Kuo, 2005:360):

$$\frac{\gamma}{\gamma - 1}\left(\frac{p_2}{\rho_2} - \frac{p_1}{\rho_1}\right) - \frac{1}{2}\left(u_1^2 - u_2^2\right) = q \tag{7}$$

Combining Equations (2) and (3) yields expressions for the velocities:

$$u_1^2 = \frac{1}{\rho_1^2}\left[\frac{\left(p_2 - p_1\right)}{\left(1/\rho_1 - 1/\rho_2\right)}\right] \tag{8}$$

or

$$u_2^2 = \frac{1}{\rho_2^2}\left[\frac{\left(p_2 - p_1\right)}{\left(1/\rho_1 - 1/\rho_2\right)}\right] \tag{9}$$

Note Equation (8) is the equation of the Rayleigh line that is capable of being derived without the use of any equation of state (Glassman, 1996:227). The combination of Equations (7), (8) and (9) form Equation (10), also known as the Hugoniot equation (Kuo, 2005:360):

$$\frac{\gamma}{\gamma - 1}\left(\frac{p_2}{\rho_2} - \frac{p_1}{\rho_1}\right) - \frac{1}{2}\left(p_2 - p_1\right)\left(\frac{1}{\rho_1} + \frac{1}{\rho_2}\right) = q \tag{10}$$

A plot of pressure (p) versus the inverse of density ($1/\rho$) given initial values of p_1, ρ_1 and q, where q is the difference in the heats of formation:

$$q \equiv h_1^\circ - h_2^\circ \tag{11}$$

and

$$h^\circ = \sum_{i=1}^{N} Y_i \Delta h_{f,i}^\circ \tag{12}$$

where Y_i is the mass fraction of the reactants and $\Delta h_{f,i}^\circ$ is the heat of formation of the reactants (Kuo, 2005:359). The resulting figure is the Hugoniot Curve which contains all possible values of $1/\rho_2$ and p_2. The curve has historically been divided into five separate regions as shown in Figure 7.

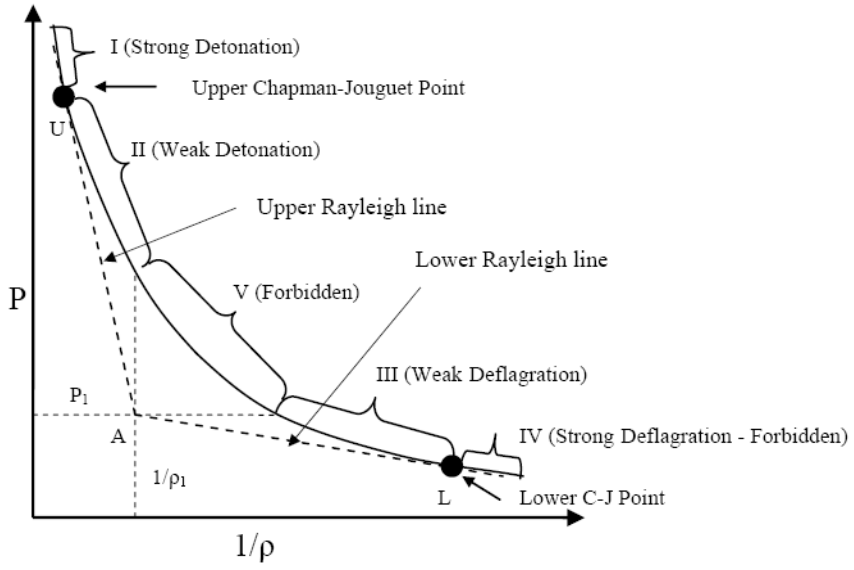

Figure 7. Representative Hugoniot curve with Rayleigh lines on P versus 1/ρ plane

The Rayleigh lines, which are drawn from the origin, A, at a tangent to the curve, create two points known as the upper (U) and lower (L) Chapman-Jouguet (CJ) points. The CJ points correspond to speeds at which detonations or deflagrations will propagate in a self-sustained fashion. The measured gaseous wave speed is the customary metric in determining the existence of a detonation in a PDE environment. The other regions (II, III, and V) are created by drawing lines of constant pressure (horizontal) and the inverse

of density (vertical) through the origin. Though the curve is representative of all possible solutions to the Hugoniot equation, not all are physically feasible or possible. The upper CJ wave speed for liquid hydrocarbon/air mixtures with equivalence ratios near one is between 1,750 and 2,000 m/s (Glassman, 1996:247). The upper CJ wave speed for the stoichiometric hydrogen-air mixture used predominantly throughout this research is known to be approximately 1971 m/s (Glassman, 1996:245).

To validate the first four regions, the ratio of Δu to u_1 can be analyzed for compression and expansion trends. The particle velocity, Δu, is obtained by solving Equations (8) and (9) for u_1 and u_2 and determining their difference. Dividing Δu by the square root of Equation (8) yields the following relationship:

$$\frac{\Delta u}{u_1} = 1 - \frac{(1/\rho_2)}{(1/\rho_1)} \tag{13}$$

This ratio is used to determine the feasibility of the output solutions.

In regions I and II, $1/\rho_2 < 1/\rho_1$ causes the right hand side of Equation (13) to be positive, yielding that u_1 is greater than u_2. This reveals that in detonations the hot gases follow the wave which agrees with the mathematical and physical understanding of compression waves and thus returns that regions I and II are feasible solutions. Further research reveals that region I is a transient state in which the detonation wave temporarily travels faster than the CJ speed; such an occurrence is known as a strong detonation or overdriven wave and is not self-sustained. Region II represents weak detonations where the pressure of the products is less than that of the pressure of the upper CJ point. Weak detonations have been found to occur only in the presence of fast acting chemical kinetics. (Kuo, 2005:361-365)

Inversely in regions III and IV, $1/\rho_2 > 1/\rho_1$ which forces the right hand side of Equation (13) to be negative. The low-velocity waves previously classified as deflagrations are present in these regions as indicated by the presence of expansion waves (Glassman, 1996:231). The strong deflagrations defined as region IV require the gas velocities relative to the wave front to be accelerated from subsonic to supersonic flow.

Lastly, region V states $p_2 > p_1$ and $1/\rho_2 > 1/\rho_1$ and according to Equation (8), the Rayleigh-line expression, u_1 would result in an imaginary number. Thus, region V is not a possible solution (Kuo, 2005:361). A result seen in this region would mandate a compression wave to overcome an impossible scenario by moving in the negative direction (Glassman, 1996:231).

Deflagration to Detonation Transition Process

The previous section detailed a one-dimensional analysis of the physics governing all combustion waves; the focus is now turned on the formation of detonation waves from deflagrations. The deflagration to detonation transition (DDT) process can best be illustrated using schematics of the tubes of the research PDE. As described previously in the PDE phase cycle discussion, a relatively long, slender tube with a single open end is filled with a vaporized fuel air mixture. A spark is deposited into the closed end of the tube and a laminar deflagration wave forms as illustrated in Figure 8.

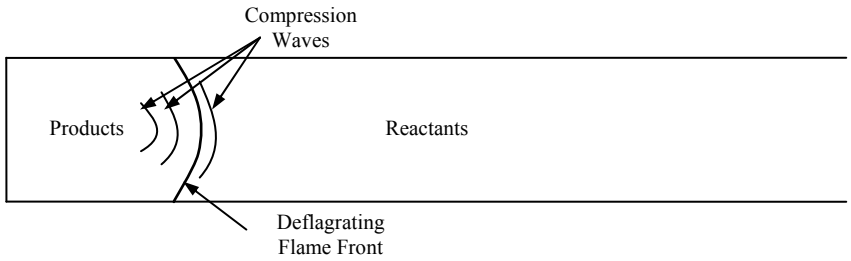

Figure 8. Deflagration wave acceleration is due to the presence of compression waves

The flame front will travel at the speed of sound based on the static temperature of the reactants as determined by the common speed of sound Equation (14):

$$a = \sqrt{\gamma RT} \tag{14}$$

where a is the speed of sound, γ is the ratio of specific heats, and R is the specific gas constant of the products.

Through the presence of compression waves, the combustion process increases the static temperature and the specific volume of the products relative to the reactants and causes the flame to increase in velocity to a point where turbulence is introduced. As the deflagration wave continues down the tube, product temperatures and specific volume continue to increase, furthering the formation of compression waves. This sequence of events causes the compression waves to coalesce into a shock wave ahead of the flame front (Kuo 2005:389). The shock wave is the source of further turbulence in the products inducing a virtual explosion within an explosion resulting in a strong spherical shock prior to the formation of the detonation wave (Kuo, 2005:389) as shown in Figure 9.

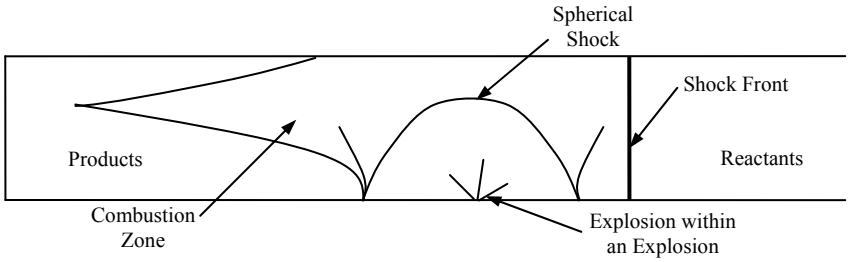

Figure 9. Shock wave forms prior to detonation wave

The spherical shock expands and reflects off the side wall and in the process forms transverse waves. A portion of the spherical shock travels through the products as a sonic retonation wave; the remainder acts to accelerate the shock front causing an overdriven detonation wave (Kuo, 2005:389) as seen in Figure 10. The overdriven wave

falls into the transient region I of Figure 7 and will eventually settle to the upper CJ speed.

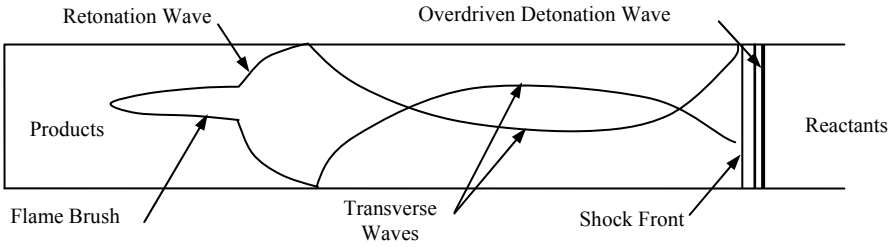

Figure 10. Detonation wave formed; overdriven at origination

The transition lengths are on the order of one meter for highly reactive mixtures and as such are not viable to eventual aircraft implementation. In order to minimize this limitation to the greatest extent, turbulence causing obstacles such as the Schelkin spirals are placed inside the detonation tubes to induce quicker DDT times and shorter DDT distances. The added turbulence and compression wave interactions cause the formation of hot spots that encourage the explosions in explosions and decrease the transition distance (Tucker, 2005). It is well known that the reduction in drag coupled with the DDT event causes the detonation wave speeds to be overdriven at the end of the spiral.

The Zel'dovich-von Neumann-Döring Model

The previous sections focused on the different properties of deflagration and detonation waves as well as the details pertaining to the formation of a detonation wave. This section delves further into the specifics of the detonation wave including the prerequisites for sustainment. Zel'dovich, von Neumann, and Döring independently developed a one dimensional model of a detonation wave known as the Zel'dovich-von Neumann-Döring (ZND) model (Kuo, 2005:381). The ZND model has become known

as the classic example of detonation propagation. Using four key assumptions (Fickett, 1979: 42):

- The flow is one-dimensional
- The shock is a jump discontinuity
- The reaction rate is zero ahead of the shock and finite behind; the reaction is also considered reversible
- All thermodynamic variables (other than the chemical composition) are everywhere in local thermodynamic equilibrium

they postulated a detonation wave can be modeled in three zones; the short duration shock wave, a longer duration induction zone, and a similarly long reaction zone. Figure 11 contains a hypothesized model in the form of a graphical representation of the important physical parameter variations (temperature, pressure and density) as a function of spatial distribution through each of the three zones.

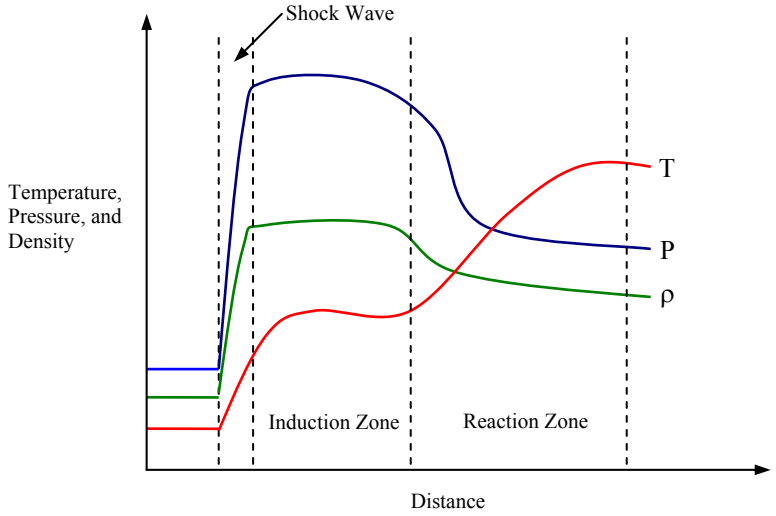

Figure 11. Generic graphical representation of the variations of physical parameters through a typical detonation wave as introduced by the ZND model

The thickness of the shock is on the order of several mean free paths and is, as mentioned, assumed to be a jump discontinuity. All three thermodynamic properties, pressure, temperature and density realize a severe spike increase as caused by the shock wave and allow for quick reaction rates which are required to sustain the detonation. It is

in essence the presence of the shock wave that allows a detonation wave to sustain. The region immediately trailing the shock wave, known as the induction zone, is where the reaction rate slowly begins to rise while there is negligible variation in the gas properties. The reaction zone however produces a large increase in specific volume that creates the compression waves also necessary to sustain the detonation front. The entire distance of all three zones is on the order of 1cm (0.39 inch) in thickness. (Kuo, 2005:381-382)

Detonation Structure

The one-dimensional detonation wave is well described through the ZND model; however an actual detonation is multidimensional in structure. Analysis of the detonation wave structure provides insight to wave propagation characteristics and also a basis for design requirements. Three-dimensional effects are most important when the width of the channel in which the detonation propagates is greater than the natural transverse-wave spacing (Fickett, 1979:298). The current experimental setup for this research however utilizes long narrow detonation tubes in which two-dimensional effects dominate the behavior of the detonation wave.

Generally speaking there are two distinct types of detonation structures; multi-head and single-head spin. A multi-head detonation structure is modeled in a long narrow channel and assumed to be governed solely by two dimensional effects. The structure of a fully developed detonation can be obtained experimentally by allowing a detonation wave to propagate along a soot-coated film in a channel. The result is a fish-scale type pattern deposited in soot on the smoke film (Kuo, 2005:384). Figure 12 illustrates an ideal representation of the structure recorded on smoke foil from the passing of a detonation wave.

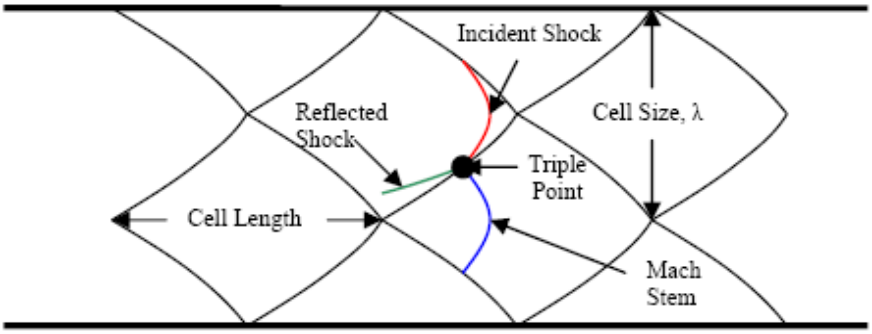

Figure 12. Idealized two-dimensional representation of a detonation's cell structure

The detonation front is composed primarily of traversing shock waves called the Mach stem and incident shock which are sustained by energy released in the combustion of the fuel-air mixture within the channel. The junction of the three waves that compose a detonation, Mach stem, incident shock and reflected shock, results in a shear discontinuity commonly referred to as the triple point. It has been postulated that the fish-scale pattern, also known as the triple point track, is due in part to the high vorticity coupled with the slip discontinuity which erases the soot as the detonation travels downstream (Glassman, 1996:255). Each individual fish-scale is known as a cell and is a characteristic of the particular detonation. As illustrated in Figure 12, the transverse spacing is the cell size while the longitudinal spacing is referred to as the cell length. Cell size (λ) is the basis for many important design criteria when performing detonation branching and in general, PDE related research.

Single-head spin detonations tend to occur most commonly in smooth circular tubes and represent the lowest stable mode of a detonation (Kuo, 2005:403). They are formed by an increased transverse wave strength that in turn amplifies the three dimensional effects associated with the detonation. The result is the formation of a detonation consisting of a single shock front with a trailing flame front that rotates about the tubes longitudinal axis. The absolute wave velocity is that of the CJ speed but a

simply measured axial velocity would be reduced due to the tangential velocity component (Kuo, 2005:403). A typical spherical wave front path associated with a single-head spin detonation is shown in Figure 13.

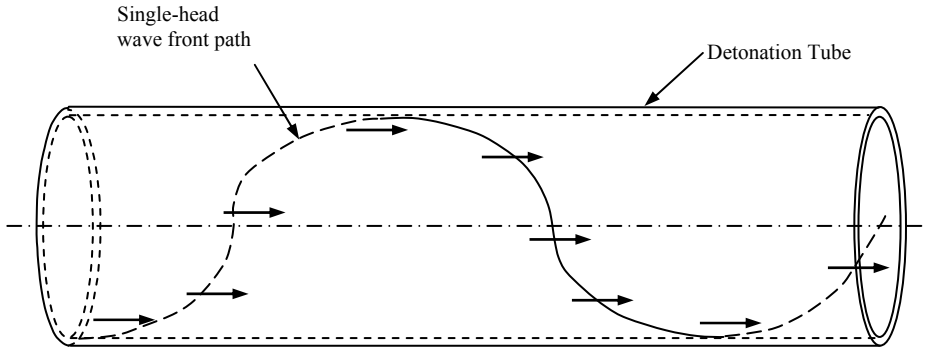

Figure 13. Illustration of the path followed by a single-head detonation wave in a tube

The onset of a single head spin detonation at a specific fuel concentration and at the minimum tube diameter can experience a phenomenon known as galloping. When a single head spin detonation encounters an obstacle, it can lose and then almost instantaneously regain its wave structure. Galloping can cause velocity fluctuations in excess of 10% of the CJ speed (Kuo, 2005:410).

Critical Diameter

As stated previously, the branched detonation tube does not create usable thrust and should be constructed in such as fashion as to reduce specific fuel consumption. The minimum tube diameter required to sustain a single-head spin detonation, also known as the critical diameter, was determined by Kogarko and Zel'dovich and later verified by Lee through the relationship:

$$\lambda = \pi d^* \tag{16}$$

where λ is the previously defined cell size and d^* is the critical diameter (Kuo, 2005:406). Equation (16) establishes the design requirement necessary for a multi-head spin detonation to transition and propagate as a single-head spin detonation through a tube of similar geometry and a restricted diameter; all of which are required during the current research involving detonation branching.

Cell Size Sensitivity

Cell size is a function of many conditions such as fuel type, dilution ratios, fuel-air ratio and wave speed. The cell sizes of various low vapor pressure hydrocarbon fuels have been determined experimentally and categorized according to the energy necessary to initiate a direct detonation, also known as the direct initiation detonation energy. A typical low vapor pressure hydrocarbon fuel combusted at a stoichiometric fuel air ratio requires approximately 1MJ of energy to obtain a directly initiated detonation (Tucker, 2005:25). The relationship between cell size and direct initiation detonation energy has been determined by a best-fit curve through the experimental data and is captured by the expression:

$$E_{DID} = 3.375\lambda^3 \tag{17}$$

where E_{DID} is the direct initiation detonation energy and λ, again, is the cell size. It should be noted that the direct initiation detonation energy varies with the cube of the cell size. Figure 14 visually illustrates the experimentally obtained data; it also shows that heavier molecular weight fuels typically result in larger cell sizes.

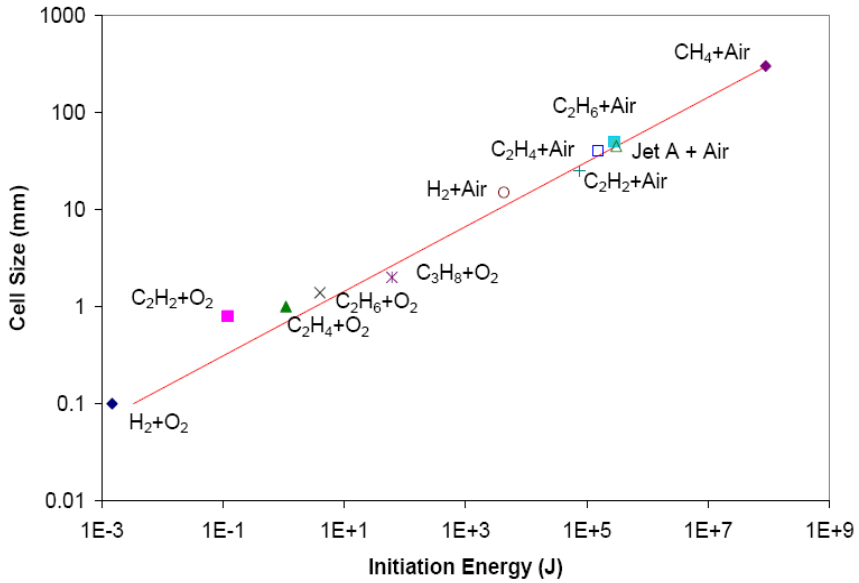

Figure 14. Experimentally determined relationship between cell size and direct initiation energy for various stoichiometric mixtures (Tucker, 2005:25)

The presence of nitrogen dilution causes an exponential increase in the cell size and initiation energy which is also captured in Figure 14. This is verified by the fact that hydrogen-air combustion has a considerably larger cell size than hydrogen-oxygen combustion and therefore, requires more energy to initiate a detonation. Related to the concepts of direct initiation energy and nitrogen dilution is equivalence ratio. Equivalence ratio, Φ, is known to be the ratio of the actual fuel air ratio to that of the stoichiometric fuel air ratio as shown in Equation (18):

$$\Phi = \frac{\left(\frac{\dot{m}_{fuel}}{\dot{m}_{air}}\right)_{actual}}{\left(\frac{\dot{m}_{fuel}}{\dot{m}_{air}}\right)_{st}} \tag{18}$$

where $\dot{m}_{fuel}$ is the fuel mass flow rate, $\dot{m}_{air}$ is the air mass flow rate and the subscripts *actual* and *st* stand for the actual and stoichiometric cases respectively. If Φ <1, the mixture is considered lean due to an excess of air, and the inherent excess nitrogen will

increase the detonation cell size. The lean limit is the lower limit of the equivalence ratio at which no combustion can take place. If $\Phi > 1$, there exists a rich environment in which the reduced percentage of air is not suitable to fully combust the fuel. Similar to the lean limit, a rich limit exists in which a large amount of excess fuel quenches the combustion process completely. Figure 15 illustrates the relationship between equivalence ratio and cell size for the primary fuel-oxidizer combination used throughout this research, hydrogen-air.

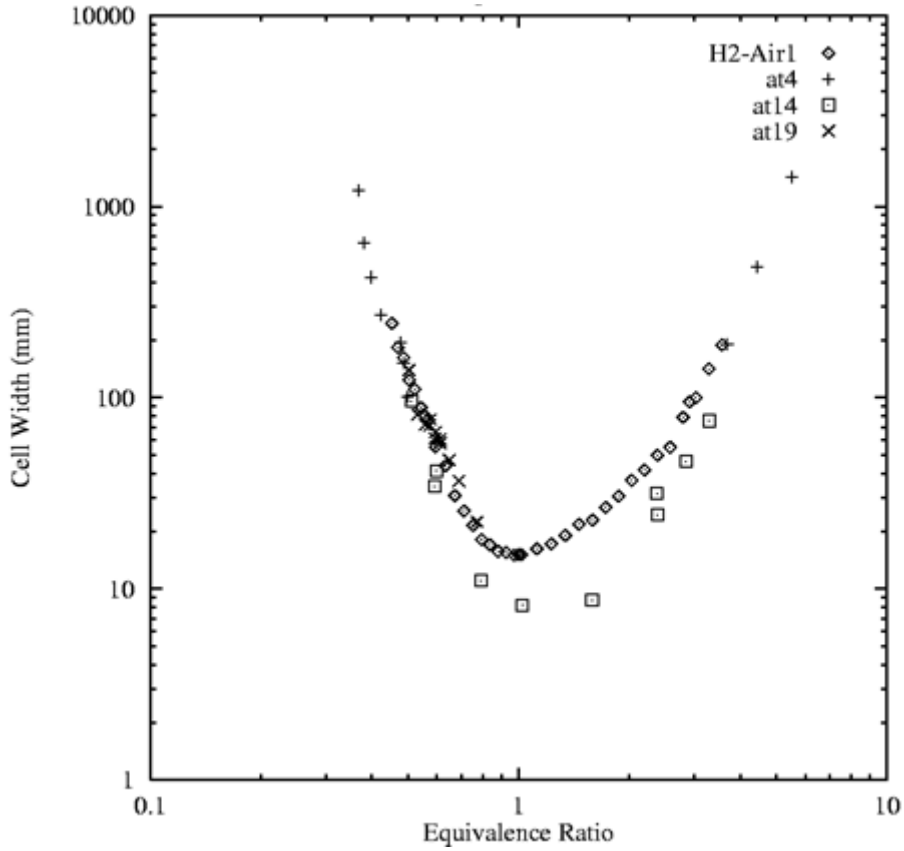

Figure 15. Cell size versus equivalence ratio for hydrogen-air (Kaneshige and Shepherd, 1997)

A couple general observations can be made from a further analysis of Figure 15: 1) the minimum cell size is obtained at or slightly above the stoichiometric equivalence ratio, 2) the slope of the curve formed by the data leads one to believe that a slightly rich mixture will not lead to an increased cell size as quickly as the alternate. This is further

verified by the fact that areas of localized lean conditions can possibly exist due to poor mixing of the fuel and air or incomplete fills.

Detonation cell size is seen to decreases when a detonation wave is in an overdriven state, which is defined as any time the velocity of the detonation is greater than that of a corresponding CJ detonation wave (Saretto, 2005). It has been experienced that an overdriven wave can result in a decrease in cell size to approximately one tenth of that associated with a CJ wave. This variation in cell size is temporary due to the transient stage of an overdriven wave discussed earlier and will increase as the wave speed decrease to the upper CJ speed; this process typically occurs within the distance of 10-15 widths of the combustion channel (Saretto, 2005).

Detonation Diffraction

The practice of detonation branching utilizes a detonation which originates from one tube to ignite a second. When the detonation exits the crossover tube, used as a means of transfer, into the larger area of the second detonation tube, it undergoes a process known as diffraction. A thorough understanding of this process is essential to the success of a direct initiation of the second tube. Diffraction is the expansion from a planar detonation to one with spherical geometry. This event is experienced during abrupt changes in area such as that when the branched detonation exits the crossover tube (Schultz, 2000:37).

As the planar detonation wave emerges, the shock front energy is reduced through the presence of strong expansion fans at the tube walls. This loss of energy can be overcome if the energy released from the combustion front is greater than that lost due to expansion effects, resulting in a successful sustainment of the detonation. When the

expansion effects dominate, the shock wave and combustion front decouple and the detonation transitions to a spherical deflagration wave. (Schultz, 2000:39)

Degrees of diffraction are categorized into three distinct cases: super-critical, near-critical and sub-critical (Schultz, 2000:5). Schultz used hydrogen detonation waves which propagated from a 25mm (0.98 inch) diameter tube into a 152mm (6 inch) square test section. The test section was equipped with transparent viewing areas which enable the ability to record shadowgraphs of diffractions in each of the three regimes.

Super-critical

The super-critical case is defined as that in which detonations successfully transition into an unconfined region. Empirical data indicates that for a detonation to survive the diffraction process from a circular tube into an unconfined space, the tube must be sized such that its diameter is at least thirteen times the cell size, or 13λ (Glassman, 1996:259). A detonation that is at least $13\ \lambda$ in size produces enough energy through the combustion process to overcome the expansion losses associated with diffraction. The shadowgraph of Figure 16 illustrates the evolution of a super critical detonation wave in which the shock wave remains connected with the combustion front and the detonation wave survives the expansion process.

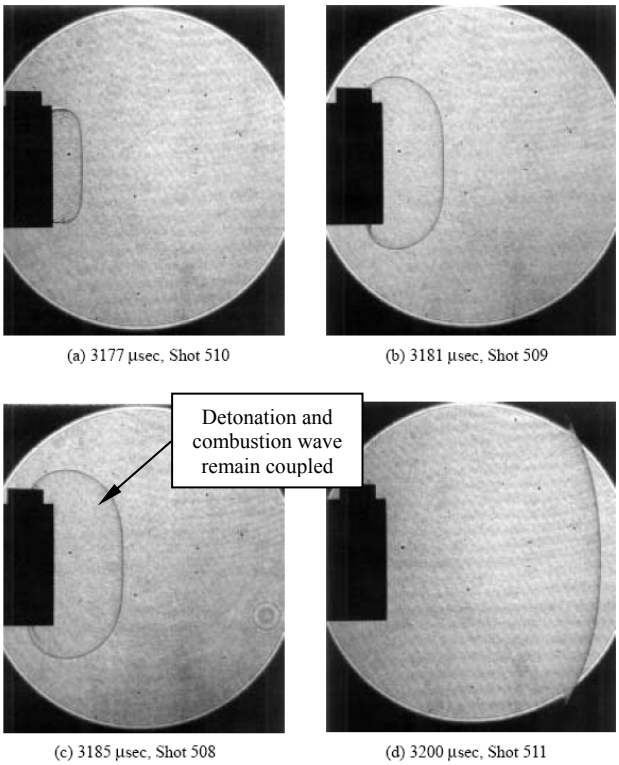

Figure 16. Shadowgraphs of super-critical detonation diffraction of hydrogen-oxygen mixture (Schultz, 2000:114)

Near-critical

The diffractions of the near-critical case results in a partial failure as the shock wave decouples from the combustion front near the edges of the detonation tube. The detachment of the shock wave from the combustion front is noted and well illustrated in Figure 17(b). Surviving portions of the detonation front however produce localized explosions which result in a highly non-uniform formation that bursts outward to re-initiate the detonation front (Schultz, 2000:116).

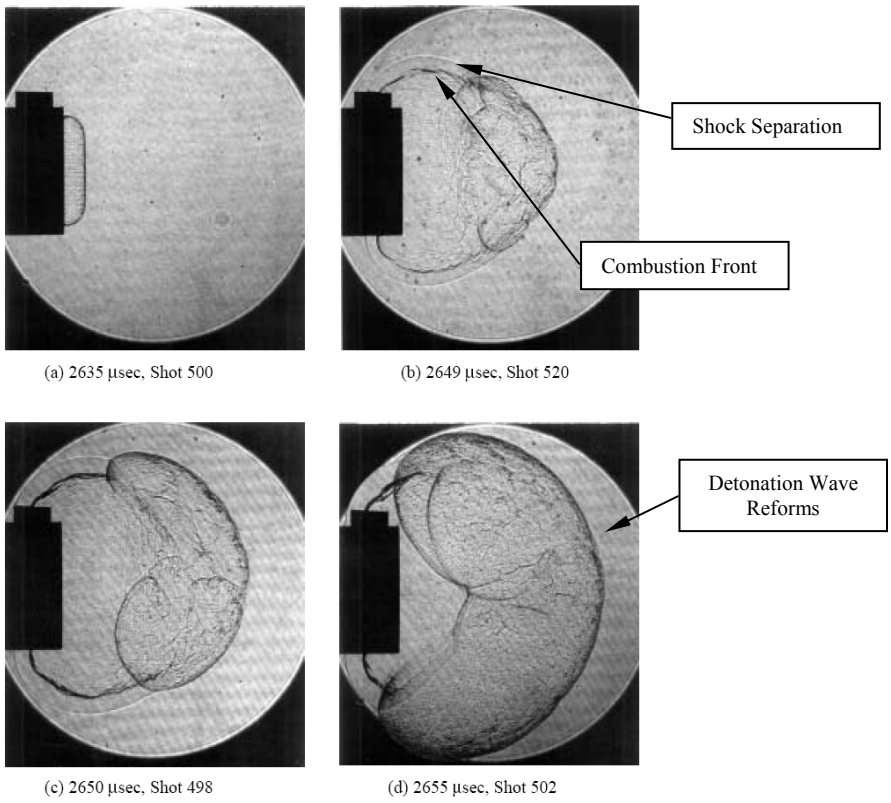

Figure 17. Shadowgraphs of near-critical detonation diffraction of hydrogen-oxygen mixture (Schultz, 2000:119)

Sub-Critical

The sub-critical diffraction case is one in which a complete failure of the detonation wave occurs. The sudden expansion causes the shock wave to decouple from the combustion front as seen in Figure 18(c) which results in a spherical deflagration wave as seen in Figure 18(d). The necessary energy is not present in the original detonation to maintain a coupling of the combustion front and shock wave.

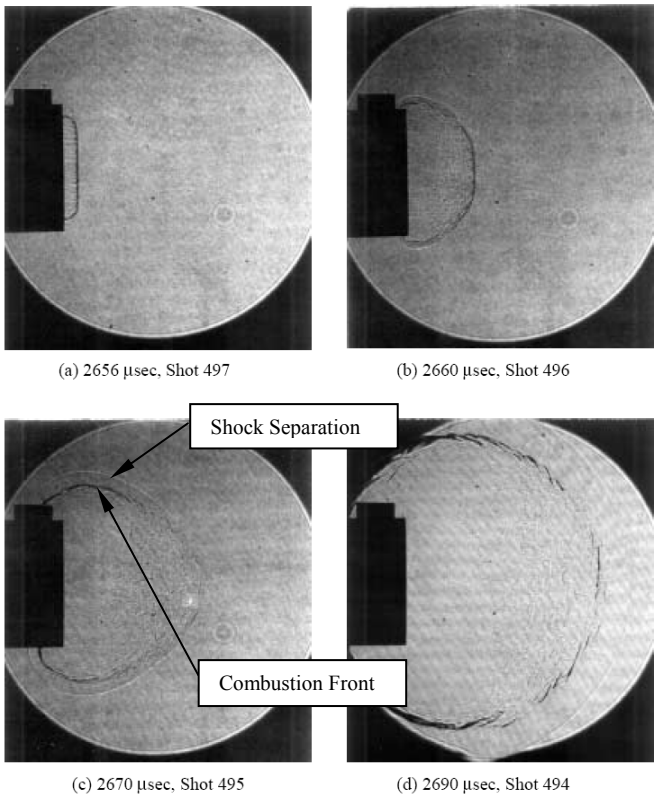

Figure 18. Shadowgraphs of sub-critical detonation diffraction of hydrogen-oxygen mixture (Schultz, 2000:117)

For all cases, the shadowgraphs indicate ignition of the hydrogen-air mixture in the expanded test section is instantaneous. The fuel is ignited by the coupled shock wave and combustion front when the diffracting detonation is of the super-critical or near-critical variety. If the entering detonation is sub-critical however, the fuel-oxidizer mixture is ignited by the combustion front of the resulting deflagration wave.

Chapter Summary

The ignition of a fuel-air mixture produces a deflagration wave which, through the aid of certain hardware, can result in a detonation wave thereby producing thrust as it exits a detonation tube. The structure of a detonation wave is known to exist in two forms; multi-head and single-head spin. Multi-head detonation waves are characterized

by cells that are the result of shear discontinuities caused by the intersection of three distinct shock waves. The tube diameter that can sustain a successful CJ wave speed detonation is directly related to the detonation cell size. The cell size depends greatly upon the properties of the fuel used, nitrogen dilution, and equivalence ratio. A detonation wave expanding into an unconfined space is categorized into three different regimes. To successfully transition a detonation without failure the wave diffraction must be super-critical or near-critical. In all cases, ignition of the fuel-air mixture in the unconfined space is considered to be instantaneous.

III. Materials and Methodology

Pulsed Detonation Research Facility (D-Bay)

The current research was conducted at the Pulsed Detonation Engine Research Facility located at Wright Patterson AFB, Dayton, Ohio, Building 71A, D-Bay. The facility is managed and sponsored by the Air Force Research Laboratory, Propulsion Directorate, Turbine Engine Division, Combustion Sciences Branch (AFRL/RZTC) with day-to-day operations handled by Innovative Scientific Solutions, Inc. (ISSI) contractors.

D-Bay is comprised primarily of the large test cell, a control room and the liquid fuel room. The research rig itself is housed in the 21,200 m^3 (748,670 ft^3) explosion proof test cell originally intended for turbojet testing which has since been retrofitted for PDE research. Similarly, the fuel and control rooms have been modified to meet the demands of the present PDE research requirements. The cell contains a static thrust stand capable of handling thrusts upwards of 267,000 N (60,024 lb_f) and acts as a base for a smaller damped test stand upon which the research PDE engine is mounted (Schauer, 2001). Directly downstream of the research PDE engine is a fan equipped exhaust tunnel to aid in the vent of combustion products during operation. The overly large facility also contains adequate workspace and tools to perform engine maintenance and minor fabrication tasks.

The test cell, fuel room and control room are all adjacent one another and are separated by two foot thick, steel reinforced concrete walls. All engine operations are regulated remotely through the use of a control panel established in *LabVIEW* control software and run on a dedicated computer. This program provides real-time monitoring, acts as a graphical user interface to all controllable engine parameters and records low-

speed data. High speed data such as wave speeds and pressure traces were collected on a separate dedicated computer operating another in house program created in *LabVIEW*. The fuel room and engine operation have the ability to be visually monitored and recorded through the use of closed circuit cameras displayed in the control room.

Air Supply System

The compressed air required for both the fill and purge cycles is provided by Ingersoll-Rand Pac Air Compressors (Model# PA 300V) capable of producing 40 m^3/min (1412 ft^3/min) of compressed air at pressures up to 6.8 atm (100 psi) individually and stored in a 4.5m^3 (159 ft^3) receiver tank (Serial# 10894, Buckeye Fabrication Co.). Due to size requirements and noise levels, the compressors and receiver tank are housed in a separate but attached room commonly referred to as the compressor room. The compressed air is routed from the compressor room into the test cell where it is split into the main and purge lines. Critical flow nozzles are installed in line with the air lines and, when a choked flow is established, provide a known mass flow rate for a given upstream pressure. This pressure is collected in both main and purge lines by upstream pressure transducers; similarly the temperature of the air is collected with upstream T-type thermocouples. These pressures and temperatures are assumed to be stagnation values and are used to determine the mass flow rate of the air in both lines. The various components of the air supply system are noted in Figure 19.

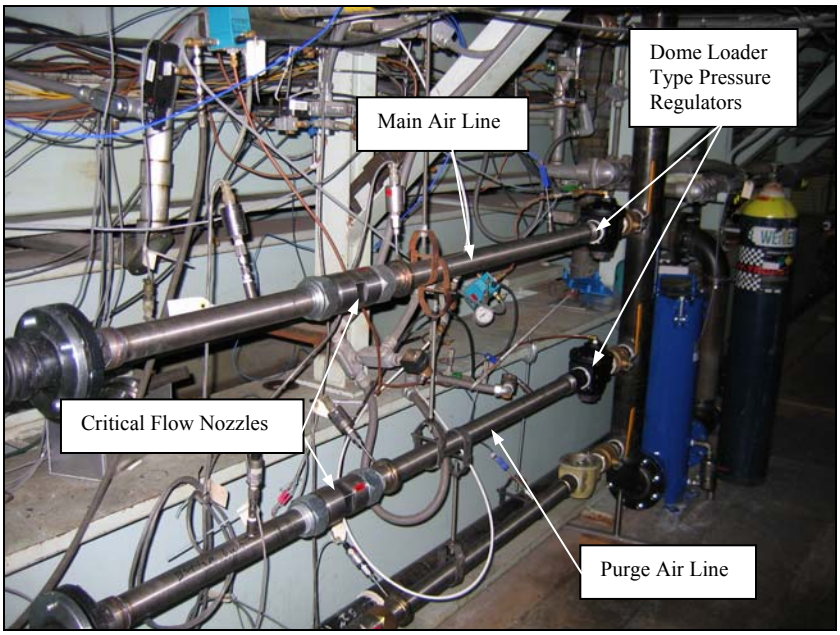

Figure 19. Research PDE air supply with important features noted

The aforementioned upstream main and purge temperature and pressures are monitored in the control room and are used by the *LabVIEW* control program to calculate the necessary air mass flow rate using Equation (19)

$$\dot{m} = \frac{(\#_{tubes})(freq)(V_{tube})(FF)(P)}{RT} \tag{19}$$

where $\#_{tubes}$ is the number of tubes used in the experimental setup, $freq$ is the engine frequency, V_{tube} is the tube volume, FF is the fill fraction, P is upstream air pressure, R is the specific gas constant for air and T is the upstream air temperature. The variables of Equation (19) are either monitored by or a user input to the control program. Tescom Electropneumatic PID controllers (Model# ER 1200) actuate dome loader type pressure regulators through the use of high pressure nitrogen to obtain the desired pressure as dictated by Equation (19). Surge tanks are located further downstream to attenuate any possible effects of compression waves as the air travels through the nozzles.

Prior to the main (often referred to as fill) and purge manifolds, the fill air is routed through a Chromalox Circulation Heater (P/N 053-500870-187) which is also controlled by the *LabVIEW* program through the use of the Chromalox temperature controller (Model# 2104). The upper temperature limit is determined by the temperature controller via a translated user input amperage in the control program.

The Pulsed Detonation Engine

The core of the PDE used in this research is a General Motors (GM) Quad 4 engine head with dual overhead camshafts. The head is equipped with two intake and two exhaust valves per cylinder as well as a mounting plate which allows a maximum of four detonation tubes to be mounted, as labeled in Figure 20.

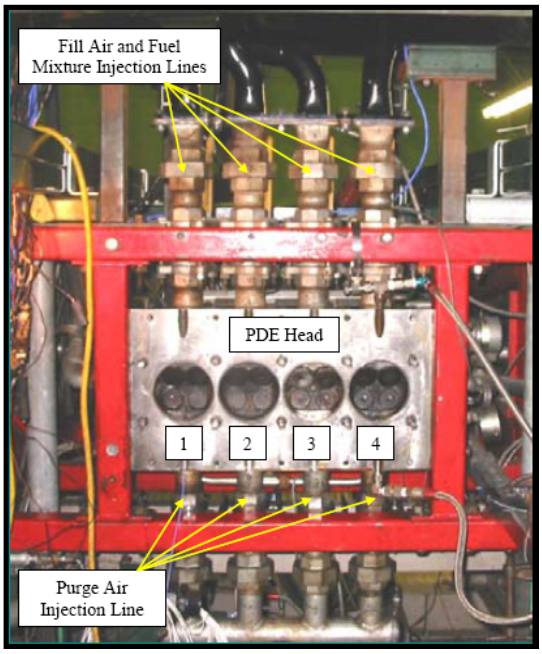

Figure 20. GM Quad 4 engine head used as the PDE research engine with the detonation tube mating points and manifold injection lines labeled

The conventional poppet style valves are mechanically actuated by their respective camshafts which are in turn driven by a variable speed Baldor Electrical motor (Model#

M4102T). The intake valves are used to provide fresh fuel-air mixture to the tubes during the fill phase while the exhaust valves similarly provide purge air during the purge phase. The fill manifold mates to the engine from above while the purge manifold attaches from below. In order to obtain the desired combination of tubes for a given experiment, each connection from the manifold (be it fill or purge) to the head is done so via a ball valve. The intake manifold is typically shrouded with insulation, which was removed for the photograph shown in Figure 20, and is designed to minimize heat loss when heating the intake air.

Engine cooling is obtained by running water from a radiator/reservoir setup via a 1.5 hp Teel electric water pump (Model# 9HN01) through the existing cooling ports in the engine head. Lubrication of the head valve train is obtained in a similar fashion only using filtered automotive oil which is pumped from a reservoir via a Viking electric oil pump (Model# FH432).

Ignition System

The heart of the PDE ignition is a 12VDC MSD brand Digital DIS-4 system used to provide the energy necessary to initiate combustion and is also controlled by the *LabVIEW* control program. A BEI brand optical encoder (Model# H25) is used to determine the angular position of the camshaft which is then used by the control computer to determine valve position and subsequent firing times. Depending upon the user input spark delay, the control program next transmits a signal to a 12 VDC MSD Digital DIS-4 ignition system through a relay box. During each fire cycle, the ignition system provides four sparks of 105-115 mJ each per tube, resulting in total ignition energy on the order of 420-460 mJ. The research engine uses modified NGK automotive

spark plugs which have the grounding electrode removed and a small piece of tube welded to the end. It can be noted now that the GM Quad 4 engine has a native firing order of 1-3-4-2.

Detonation Tubes

The hardware for the research presented consisted primarily of two detonation tubes mounted to consecutive firing order positions 1 and 3 on the engine head. The detonation tubes will be referred to interchangeably by their corresponding head locations as well as by their function as primary and secondary detonation tubes. Tube one, the primary detonation tube, is the spark ignited detonation tube used throughout this research with a sole purpose of producing repeatable and consistent detonations. The secondary detonation tube, number two, is the branched ignited tube. A later examined crossover tube allows detonation branching to occur from near the tail of the spark ignited tube and directs the detonation towards the closed (or head) end of the secondary tube. The material used to construct the primary and secondary detonation tubes consisted of Schedule 40 two inch (nominal dimension) piping. The crossover tube was fabricated from one inch by 0.065 inch wall thickness stainless steel tubing and was chosen for the crossover tube to meet the minimum diameter criterion of a single-head spin detonation as determined by Equation (16). In each case, off the shelf materials were utilized to minimize expense and to expedite the fabrication process. The detonation tubes attach to the engine with 0.5 inch steel mounting plates that have been threaded to accept the detonation tubes and are notched to mate the head bolt pattern. The connections were sealed with a stock head gasket which was placed between the mounting plate and the head.

Spark Ignited Tube

There are five major components that combine to construct the primary detonation tube: a mounting plate, steel pipes, a spiral, a T-like junction and a reducer. The pipe components are, as mentioned, nominal 2 inch schedule 40 steel pipes which are threaded with a standard male national pipe thread taper (MPT). As the primary source of fabrication materials was the onsite supply, ion probe ports are located seemingly randomly along all pieces that were not constructed specifically for this research. The only wave speed recorded from the spark ignited detonation tube was that which will be referred to as the pickup wave speed. This was the wave speed recorded from ion probes located on either side of the T-like component which is where the detonation branches into the crossover tube. All other existing ion probe locations were capped during the runs. The detonation was obtained through the use of a Schelkin-type spiral strategically placed such that the overdriven wave obtain at the end of the spiral was present at the pickup location. It has been shown that detonation branching is more successful when conducted in the presence of an overdriven wave which has the characteristic of a reduced cell size as mentioned earlier (Panzenhagen, 2004). The final piece is the reducer which resulted in a 25% reduction in tail-end diameter and an unquantified pressure rise within the tube.

Crossover Tube

The crossover tube is approximately 51 inches long and is constructed of one inch by 0.065 inch wall thickness stainless steel tubing. The wall thickness resulted in an

internal diameter of approximately 0.87 inches. It is equipped with Swagelock compression fittings on either end; one mates to the T-like fitting on the primary detonation tube while the other completes the connection to the union piece near the head of the secondary detonation tube shown in Figure 21. It is equipped with numerous ion probe ports which offer many available combinations through which to obtain wave speed measurements.

Detonation Ignited Tube

The secondary detonation tube is similar in construction to the primary detonation tube. One of the few differences is the lack of any type of detonation initiating hardware. Second, is the innovative method in which the transferred detonation is introduced to the secondary tube. The crossover tube was joined to the second detonation tube in a manner that forced the flow to undergo two consecutive 90 degree turns. The section of the secondary tube to which the crossover tube is joined is again a two inch Schedule 40 pipe that was attached to the head via a mounting plate and equipped with a Swagelock compression fitting for the crossover tube to connect. This transition piece, seen in Figure 21, forces the transferred detonation to enter the secondary tube perpendicular to the flow.

Figure 21. Union point of crossover tube and secondary detonation tube

The remainder of the secondary tube was composed of steel union fittings, other various lengths of Schedule 40 piping equipped with ion probe ports (to make it approximately of equal length as the primary detonation tube) and is finished with a reducer similar to that of the primary detonation tube. As mentioned, a stock engine head gasket was used to create a seal between the engine block and the detonation tube mounting plates. A picture of the setup, sans reducers, is shown in Figure 22 and a schematic of the setup is given in Figure 23.

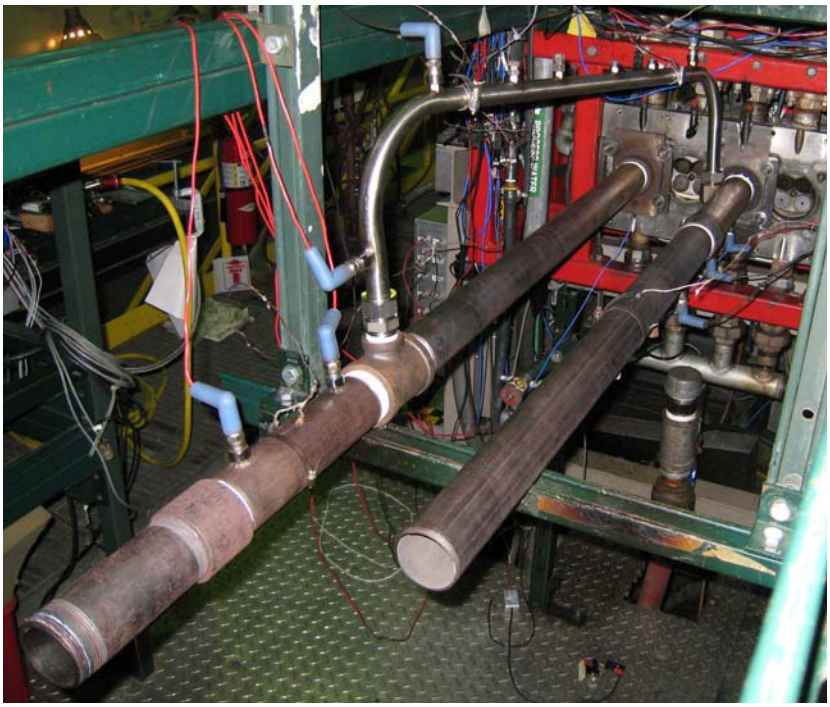

Figure 22. Branch detonation test setup using engine head locations one and three

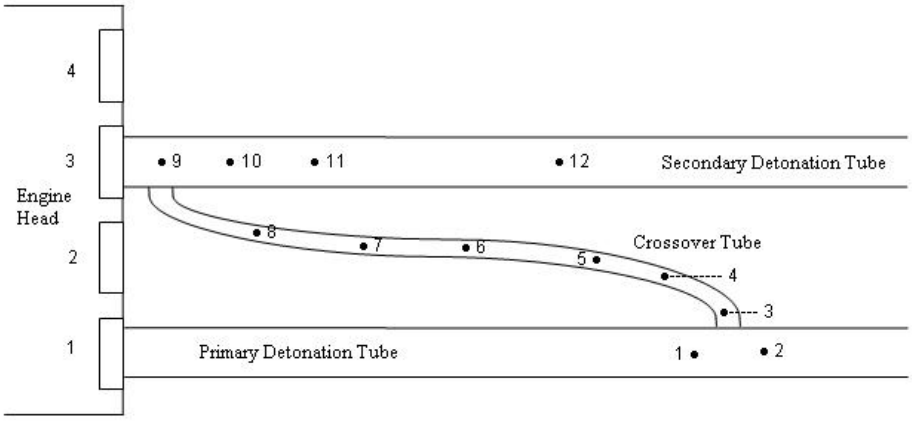

Figure 23. Test setup schematic with approximate locations of ion probes indicated

Engine Timing

As mentioned previously, the firing order of the tube locations as based on the valve operations via the camshaft is 1-3-4-2 with each tube location being 90^{o} of camshaft rotation out of phase with its predecessor. Also, the spark delay (SD) has been defined as the time allotted between the fill valve closure and the spark deposition in the primary detonation tube. In order to prevent backfiring into either the purge or fill manifolds, a SD was selected such that the transferred detonation would not arrive in the secondary tube until the fill valve had closed in the secondary tube. The two cylinders chosen are next to each other in the engine firing order, thereby allowing the detonation from the primary tube to act as the ignition source for the secondary tube. The SD is directly related to the engine frequency (*f*) of which various values are tabulated and displayed in Table 2. The majority of the data collected during this research was conducted at an engine frequency of 10Hz (highlighted in Table 2) which resulted in an approximate SD of 25 milliseconds.

Table 2. Various spark delays shown vs. engine frequency

Frequency (Hz)	Time/Cycle (ms)	Time/Phase (ms)	Spark Delay (ms)
2	500.000	166.667	125.0
4	250.000	83.333	62.5
6	166.667	55.556	41.7
8	125.000	41.667	31.3
10	100.000	33.333	25.0
12	83.333	27.778	20.8
14	71.429	23.810	17.9
16	62.500	20.833	15.6
18	55.556	18.519	13.9
20	50.000	16.667	12.5
22	45.455	15.152	11.4
24	41.667	13.889	10.4
26	38.462	12.821	9.6
28	35.714	11.905	8.9
30	33.333	11.111	8.3
32	31.250	10.417	7.8
34	29.412	9.804	7.4
36	27.778	9.259	6.9
38	26.316	8.772	6.6
40	25.000	8.333	6.3

Instrumentation

The instrumentation for each of the tests performed remained relatively constant with small variations concerning the combination of ion probes used; the head pressure transducers, and thermocouples were consistent throughout. The temperature of the fill fuel-air mixture was measured directly upstream of the entrance to the PDE using a 1/8 inch T-type thermocouple. Similarly, the temperature of the purge air was monitored; both to ensure an immediate ignition cutoff should the temperature spike due to a backfire.

A PCB pressure transducer was situated in the head cavity of both detonation tubes; S/N 15010 and S/N 17994 primary and secondary respectively. The data obtained was used by the post-processing program (discussed later) to determine ignition time in the spark ignited detonation tube and to verify the arrival of detonations to the secondary detonation tube. These particular transducers were previously calibrated and it was determined that they exhibited a pressure to voltage conversion factor of 1037 and 883 psig/V respectively.

In a PDE environment, thermal shocks accompany the pressure pulses of detonations measured by the pressure transducers. Most pressure sensors are sensitive to these thermal shocks, as were the PCB pressure transducers used in this research. The sensor case expands with the heat, resulting in a reduction of the preload force on the internals of the sensor and causes a negative-signal output. This effect was partially alleviated through the application of a silicon RTV sealant as a thermal protection coating. Even with such precautions however, the negative-signal output was realized

and as will be mentioned again later, the resulting output was used in a qualitative/comparative manner only. (PCB Piezotronics, 2008)

The ion probes used are simply automotive spark plugs acting as capacitors. Approximately five volts are applied to a probe and as the ions present in the combustion wave pass, the circuit is completed and the voltage is discharged. The voltage traces of numerous ion probes are recorded by the high-speed computer using a custom *LabVIEW* program along with the spark and head pressure data which can be used to determine various performance parameters such as ignition time, wave speeds, and DDT time. Figure 24 is a photograph showing the placement of the head pressure transducers and a limited sampling of the ion probes and locations.

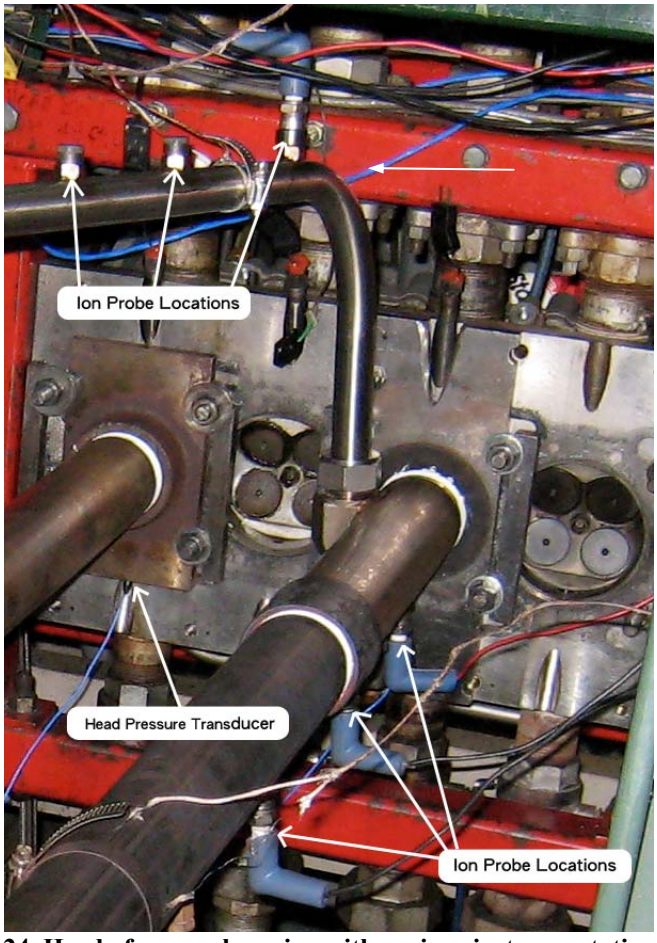

Figure 24. Head of research engine with various instrumentations noted

Data Acquisition

The *LabVIEW* program collected data at a rate of one MHz which captured 500,000 individual data points for up to 12 channels during a one-half second run duration. The typical 10 Hz engine operating frequency resulted in the capture of three to four complete detonation cycles per run. The output of the high-speed data acquisition program is a binary file containing a continual string of pulse data. Useful data, wave speeds and pressure traces in this case, are extracted from the raw files utilizing a separate in-house *C++* program named *PT Finder* (see Appendix A for more information).

Test Procedures

Prior to testing, the fuel and air mass flow rates were calculated and the corresponding flow number and critical flow nozzles were installed. Transformers were energized and nitrogen bottles were opened to facilitate cooling, lubrication and control of the research engine. The air compressor was initiated and a blown down of the main air lines was conducted to prevent settled rust and water from damaging any components of the PDE. From the control room the critical flow nozzles, number of tubes present, tube volume, desired equivalence ratio, purge and fill fractions were entered into the low-speed control computer. The engine was brought to the desired operating frequency and the spark delay was set through the low-speed *LabVIEW* control program in the control room. The air, without fuel, is then actuated and permitted to flow through the fill and purge lines into the PDE.

To commence engine firing, the low-speed data collection system equipped on the control computer was initiated, the igniters were energized and the last chance fuel valve was opened to allow fuel flow. Upon the steadying of the fuel mass flow rate, combustion began in the detonation tubes. The equivalence ratio was then adjusted by increasing or decreasing pressure in the fuel line using a previously described Tescom dome-type pressure regulator. Generous amounts of data were collected by the high speed computer and are presented later. Upon completion of data collection, the last chance valve was closed and the engine continued to run until the remaining fuel in the line was consumed. The ignition source in the primary detonation tube was discontinued and the engine was shutdown in approximately the reverse order of startup.

IV. Results and Analysis

Due to limitations of the data acquisition system, testing was performed in various phases. The system, as mentioned, is capable of obtaining twelve channels of data simultaneously. Head pressures in both tubes and the spark, which was deposited in the primary detonation tube only, were recorded for every run. This limited the number of channels for acquiring wave speed measurements from ion probes to a maximum of nine. Also for every run, the pickup wave speed was recorded to ensure that the overdriven case was obtained, leaving seven channels for additional ion probes. As such, the first phase of research was limited to data acquisition from only the pickup location and along the crossover tube. These data were used to determine the nature of the detonations produced in the primary detonation tube and also those captured in the cross-over tube by detonation branching. It should be noted now that the red dashed lines in the latter wave speed plots indicate the span of the crossover tube.

Subsequent runs focused on locations further downstream along the path of the branched detonation. Numerous parameters were held fast for all runs; Table 3 contains a conditions matrix which summarizes those varied, including ion probe locations used.

Table 3. Conditions matrix housing setup parameter for various test runs

Run Number	Equivalence Ratio (φ)	Ion Probe Location Number	Primary Tube Reducer	Secondary Tube Reducer
1	1	1 - 8	Y	N
2	1	1, 2, 7 - 12	Y	N
3	1	1, 2, 7 - 12	Y	Y
4	0.9	1, 2, 7 - 12	Y	Y

The wave speeds reported throughout this research are the average wave speeds of the midpoint between two ion probes and as such are reported at these midpoint locations. The ion probes, and similarly the wave speeds reported later, are located relative to their downstream distance from the head of the primary detonation tube and are recorded in Table 4.

Table 4. Distance of ion probes from the closed end of the primary detonation tube

Ion Probe Location Number	Distance from Head 1 (inches)
1	35
2	42
3	42
4	51
5	57
6	67.25
7	72
8	78
9	92
10	95
11	98
12	105.25

Unless other wised noted, the following engine control variables were held constant throughout the various phases of testing. The equivalence ratio (φ) was maintained at the stoichiometric value in order to reduce the detonation cell size (λ), as illustrated in Figure 15 of Chapter II, which results in an increase of the branched detonation pick-up success rate. The fill fraction (FF) and purge fraction (PF), both defined above, were held constant at 1.5 and 0.7 respectively. The over-fill (FF>1) was used to ensure complete filling of the crossover tube. Testing yielded that a fill fraction of one did not allow for the crossover tube to fill as indicated by wave speed measurements. In typical PDE operation however, the fill fraction should be minimized so as to reduce

unnecessary fuel consumption. A similar relative increase in the PF over a non-crossover setup was used. The engine frequency (*f*) was held at a constant 10 Hz for all runs.

Prior to the presentation of data, various terms used throughout the discussion will be defined. Detonation branching is the process of splitting a detonation formed in the spark ignited tube into the crossover tube. Spark ignition is the process of igniting combustion through the use of a spark plug. Direct initiation, as discussed here, is the process of a detonation wave successfully sustaining from the crossover tube into the secondary tube with no necessity of a second DDT event.

Crossover Tube Wave Speed Measurements – Run 1

Wave speeds in the detonation and crossover tubes were measured using ion probes in locations shown previously in Figure 23. Two modified renditions of this schematic will be presented with the various ion probe locations identified as outlined in Table 3. Figure 25 houses such said schematic illustrating the ion probe locations for Run 1 which focused on the crossover tube wave speed measurements.

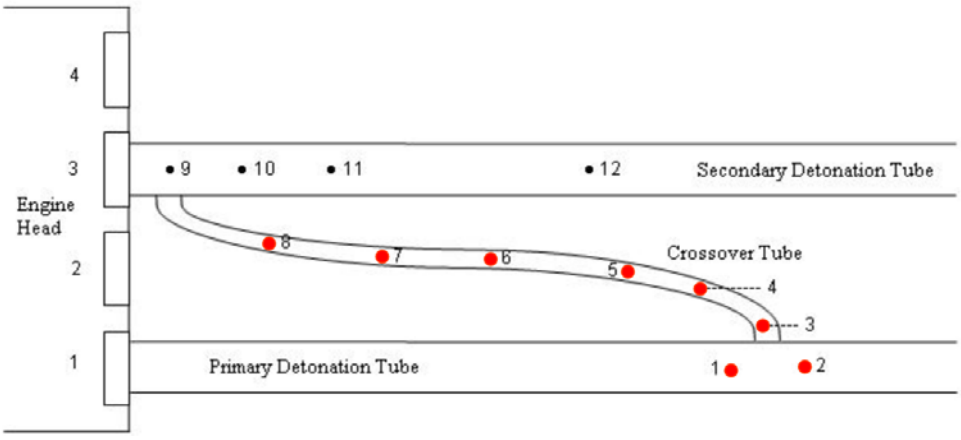

Figure 25. Schematic of ion probe locations used during crossover wave speed measurements

As explained previously, the success rate of detonation branching is increased when the branching occurs in the presence of an overdriven detonation. The CJ wave speed for the stoichiometric hydrogen-air mixture primarily used throughout this research is known to be approximately 1971 m/s (Glassman, 1996:245). The characteristics and overall stability of the detonations in this research are extrapolated primarily from wave speed measurements collected and presented throughout. As mentioned in Table 3 , only the primary detonation tube was equipped with the tail-end area restrictor for Run 1. Initially, determining the success of detonations throughout the length of the crossover tube was of most importance; these data are presented in Figure 26.

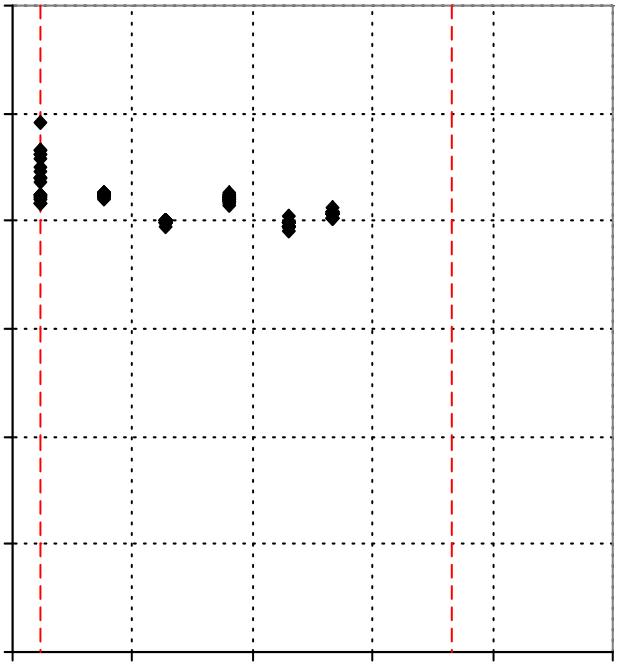

Figure 26. Run 1 wave speeds collected along the crossover tube as a function of distance from the head of the primary detonation tube

The overdriven state at the pickup location was obtained as indicated by the local average wave speed of 2394 m/s, approximately 21% greater than the CJ value. The

current engine parameters in conjunction with the primary tube restrictor produced consistently strong detonations both at the pickup location and also through the measure section of the crossover tube. Physical limitations of the test setup prohibited collecting wave speed measurements closer to the delivery end of the crossover. The wave speed throughout the crossover tube was slightly lower than the pickup speed, averaging 2093 m/s. The lowest average wave speed recorded for a single location along the crossover tube was 1962 m/s; less than the one-half percent away from the CJ speed mentioned previously. With the belief that strong detonations were present throughout the length of the crossover tube and being delivered to the union with the secondary detonation tube, the focus of wave speed measurements was moved further downstream. Please refer to Appendix A for more information on wave speed calculations.

Secondary Detonation Tube Wave Speed Measurements

The remaining data presented is that obtained with a focus on the secondary detonation tube. The ion probe locations used for the remainder of the runs are illustrated in the schematic of Figure 27.

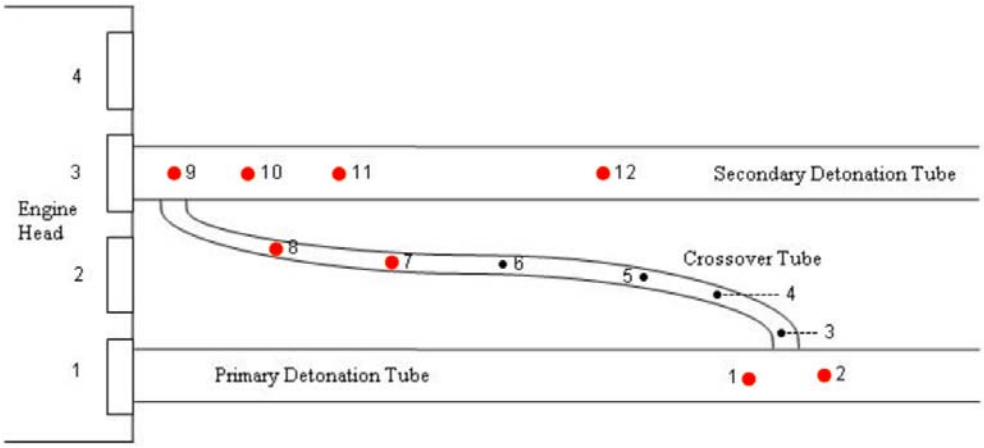

Figure 27. Schematic of ion probe locations used during secondary detonation tube wave speed measurements

The data presented in this subsection results from moving the ion probes at locations three through six in the crossover tube to locations nine through twelve in the secondary detonation tube; this change is visually illustrated in Figure 27.

Run 2 – Initial Measurements in Secondary Detonation Tube

At this time, no changes other than those to ion probe locations were made concerning the physical geometry or engine parameters. The primary detonation tube was again equipped with the restrictor resulting in a 25% tail-end reduction in diameter. As mentioned, this caused an un-quantified pressure rise in the primary detonation tube and was seen to further aid in the successful detonation branching to the cross-over tube. The eight ion probe locations used as shown in Figure 27 resulted in the production of five distinct wave speed measurements for the passing of every combustion event through the following combination of ion probe locations: 1-2, 7-8, 9-10, 10-11 and 11-12. These data are present in Figure 28 which again displays the consistently overdriven detonations at the pickup location with average wave speeds of 2255 m/s. The conditions near the

delivery end of the crossover tube were also similar to those observed during Run 1 with wave speeds averaging 2042 m/s.

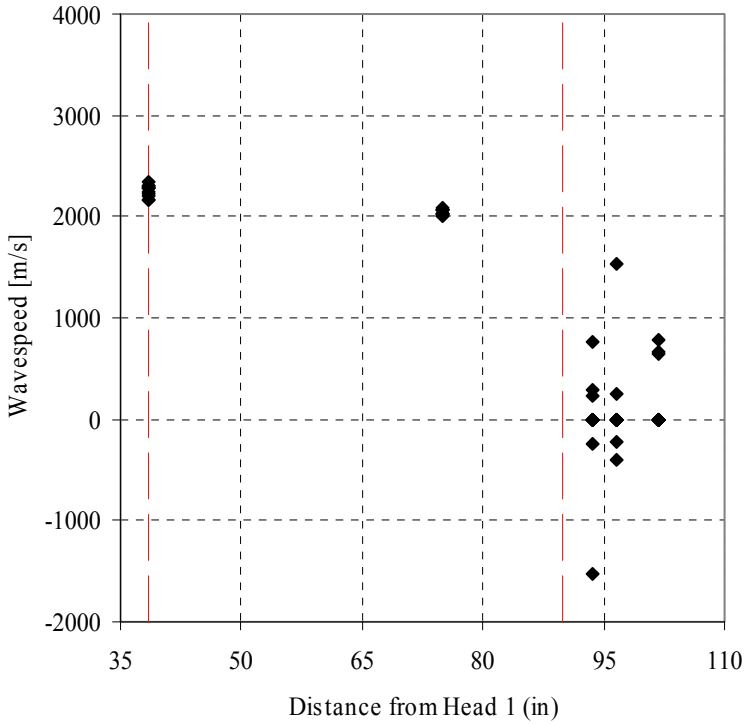

Figure 28. Run 2 wave speeds from the pick-up, crossover, and secondary detonation tube as a function of distance from the head of the primary detonation tube

The low and negative wave speeds observed in the secondary tube (to the right of the second red line) are due to weak ion probe drops and indicate a possible decoupling of the shock and combustion front upon expansion into the secondary detonation tube. Only three sets of data were collected with this setup, during which eleven detonation traces were recorded. The limited amount of data for this phase was due to the intermittent analysis conducted during the collection of data which made it apparent that the desired outcome was not being obtained.

Run 3 – Second Measurements in Secondary Detonation Tube

The wave speeds observed in the secondary detonation tube without restrictors present (not shown) were poor, as were the results shown in Figure 28 with only the primary detonation tube tail-end diameter reduced. This led to the inspiration of placing restrictors on both the primary and secondary detonation tubes. The 25% reduction in tail-end diameter to the second tube was the only change from the previous setup of Run 2; all other variables were maintained at current conditions. This resulted in the first successful detonations seen to travel from initiation, through the crossover tube and transition into the secondary detonation tube without the necessity of DDT hardware in the secondary tube. These data are presented in Figure 29 but as noted, must not be used out of context.

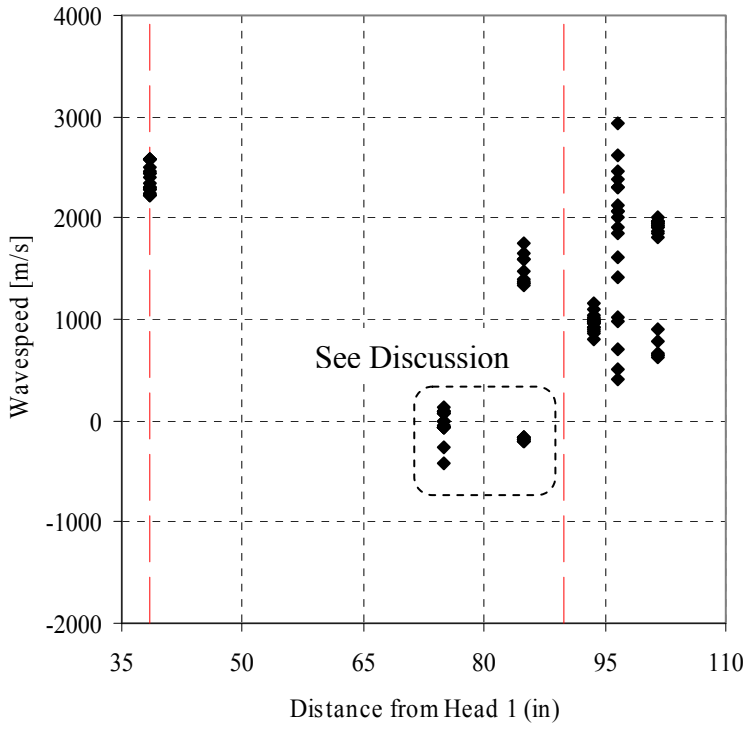

Figure 29. Run 3 with CJ wave speeds seen in secondary detonation tube are indicative of successful detonation transitions

There are nineteen individual wave traces represented in the Run 3 data; thirteen traces in which the final measured waves speeds were 1800 m/s (91% of the CJ value) or greater. Downstream of the crossover at the 93.5 inch axial location, it appears that the detonations are initially slowing to ~1000 m/s. One possible cause of this occurrence could be due to a partial shock/combustion decoupling event as discussed earlier with diffraction. The broad range of wave speeds at the next axial measurement location indicates a possible re-initiation event for some percentage of the cycles. At the final wave speed measurement location of ~102 inches, the individual wave traces appear to have separated into detonations with wave speeds greater than 1800 m/s or deflagrations with speeds below 1000 m/s. The average wave speed at pick-up for the data present in Figure 29 is 2382 m/s and the final most downstream wave speed including all values displayed averaged 1535 m/s.

There is concern pertaining to the wave speed measurements observed in the crossover tube which are denoted in Figure 29. While the pick-up wave speeds exhibit the same overdriven tendency presented in Run 1 and Run 2, all the wave speeds at the 75 inch location and approximately half of those at the 85 inch location are either negative or very near zero. There is no direct correlation between these low wave speed measurements and the ultimate success or failure of the detonation in the secondary tube (as will be evident in a sort of the Run 3 data), indicating that the low wave speeds recorded do not signify a complete failure of the detonation in this case.

Ion Probe Trace Analyses

An examination of the wave speed traces of individual detonations yields that near zero and negative wave speeds were the results of weak ion probe readings. The final wave speed measured in the crossover tube (shown at the 75 inch axial location) is a product of two ion probe measurements: one at 72 inches and the other at 78 inches from the head of the primary detonation tube, locations 7 and 8 from Figure 27 respectively. If the probe at the 72 inch location does not experiences a sharp voltage drop, the program used to determine wave speeds will not properly calculate the wave speed shown at the 75 inch location only. However, if the ion probe at the 78 inch location experiences a weak drop, the wave speeds shown at both the 75 inch and 85 inch locations will be improperly calculated due to the same explanation. These weak ion probe readings are possibly due to a lower rate of ions being produced by the combustion process, as would be the case in a deflagration rather than detonation combustion. Oran et al. have demonstrated the presence of un-reacted gas pockets in discrete locations behind a marginal detonation wave. In this case, the crossover tube diameter is small enough that the detonation wave can be classified as marginal, and it is theorized that the low or negative wave speeds resulted from relatively slow ion formations due to deflagration occurring within these un-reacted gas pockets.

The ion probe traces collected near the end of the crossover tube for two combustion events were next analyzed; one with a reasonable wave speed measurement and the other not (i.e. negative or extremely low), as deemed by the computer output wave speed measurements. The first resulted in a measured wave speed of 2005 m/s at the 75 inch axial location. Figure 30 contains the ion probe voltage traces from probe

locations seven and eight of Figure 27 as a function of time. The abrupt drops in voltage allow the computer program to determine the wave speeds as described in greater detail in Appendix A.

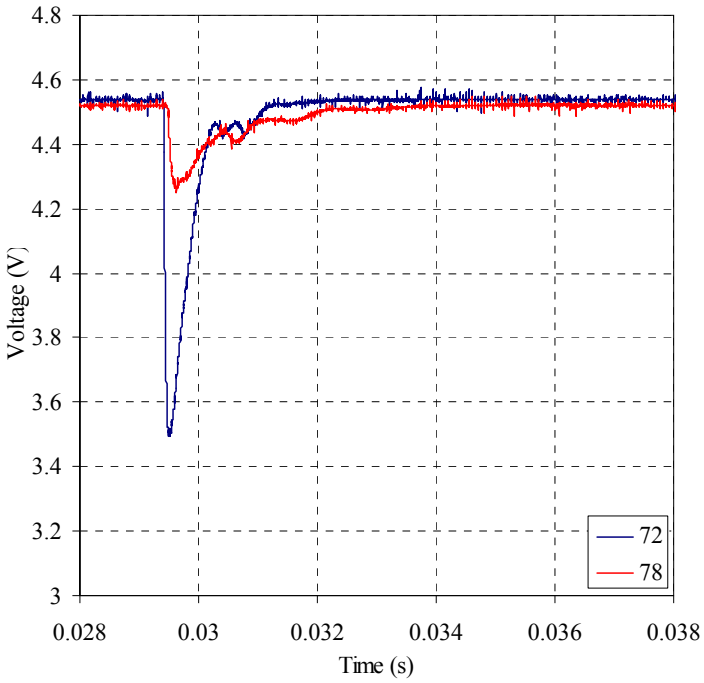

Figure 30. Ion probe voltage trace resulting in a calculated wave speed of 2005 m/s at the end of the crossover tube as a function of time

As mentioned, the second analyzed wave speed trace resulted in an unrealistic wave speed. In this case, the output value was just slightly negative at the 75 inch axial location. The reason becomes apparent upon inspection of the ion probe voltage traces shown in Figure 31 which contain no such abrupt drop necessary for the wave speed calculation. The combustion event for this figure passed near the 0.03 second time mark as indicated by the other ion probe traces (not shown for clarity purposes); however the majority of the voltage drop occurred approximately 2 milliseconds later. This may be

the deflagration of the suspected unreacted gas pockets formed behind the marginal detonation wave discussed above.

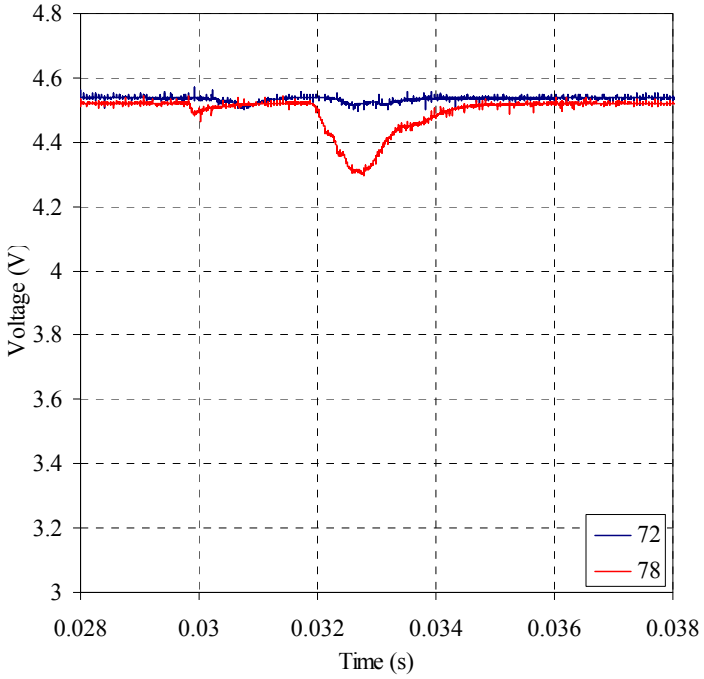

Figure 31. Ion probe voltage trace resulting in an unrealistic, negative calculated wave speed at the end of the crossover tube as a function of time

Run 3 (sort) – Chapman-Jouguet Wave Speeds in Secondary Detonation Tube

A sort was conducted from the data collected during Run 3 to show only those combustion events with a final wave speed in the secondary tube (between locations eleven and twelve of Figure 27) greater than 1800 m/s; the result is Figure 32. This criterion was met by 13 of the 19 individual combustion traces. The successful unaided detonation transition occurred only when both detonation tubes were equipped with the tail-end restrictors. These data confirm the belief that the low and negative wave speeds recorded near the end of the crossover tube do not directly correlate to the downstream

wave speeds. The pickup detonations presented here are again overdriven to an average of 2382 m/s while the final wave speeds measured in the second tube are 1915 m/s, very nearly the recognized steady-state detonation CJ speed.

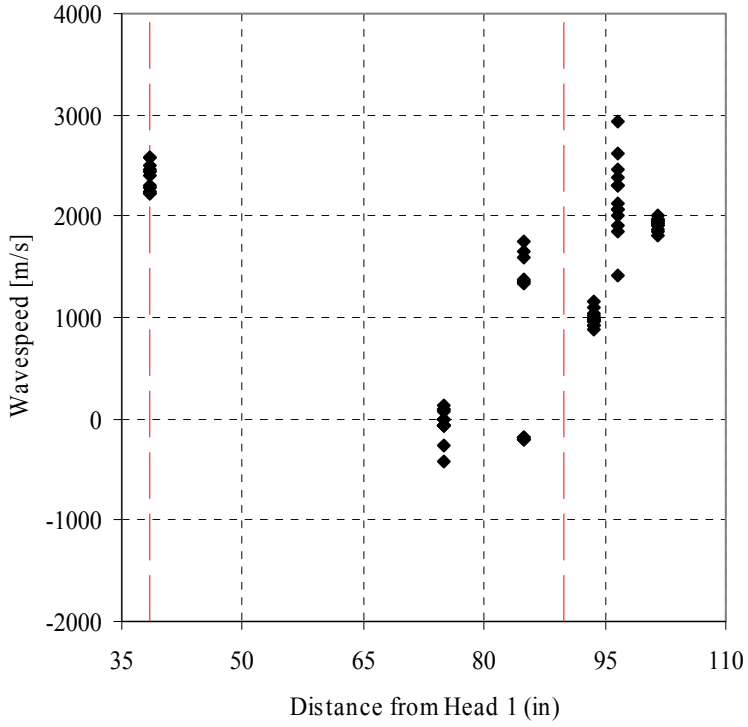

Figure 32. Detonation traces from Run 3 with final wave speeds in the secondary detonation tube greater than 1800 m/s

Head Pressure Analysis of Branched Detonations

Successful Detonation Transfer

In order to obtain more confirmation of the successful direct initiation, the head pressure traces recorded during every run were analyzed. As is customary when analyzing pressure traces in a detonation environment, the pressure is plotted as a function of non-dimensional time. This non-dimensional value was obtained using another time known as the Chapman-Jouguet time (t_{CJ}) which is defined as the tube

length divided by the CJ wave speed. The data presented in Figure 33 is that obtained during a combustion event in which the final measured wave speed was at or very near the CJ wave speed for the stoichiometric fuel-air mixture used during Run 3.

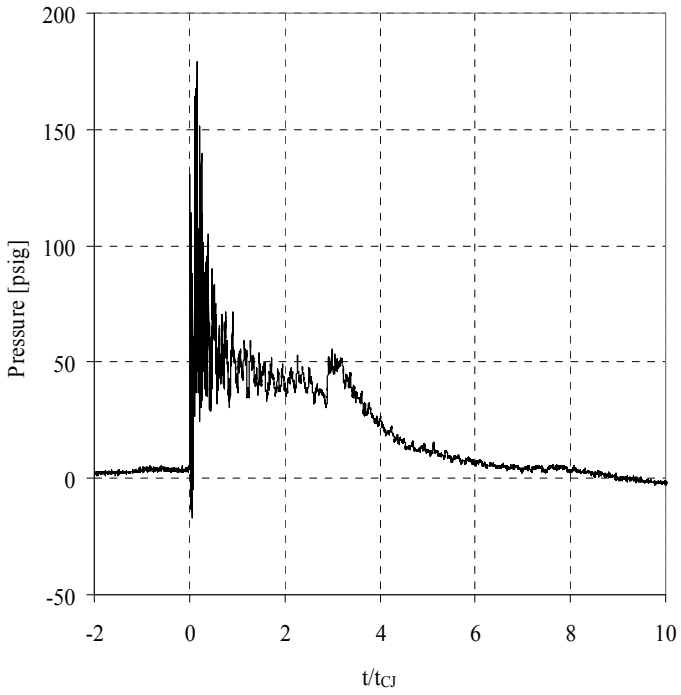

Figure 33. Secondary detonation tube head pressure trace as a function of non-dimensional time for a successful direct initiation

The corresponding wave speeds of the detonation that produced this pressure trace are one of those contained in the sort of Run 3 (Figure 32) data and are presented individually in Figure 34. The overdriven case is again obtained at the pickup location with a wave speed at this location of 2577 m/s.

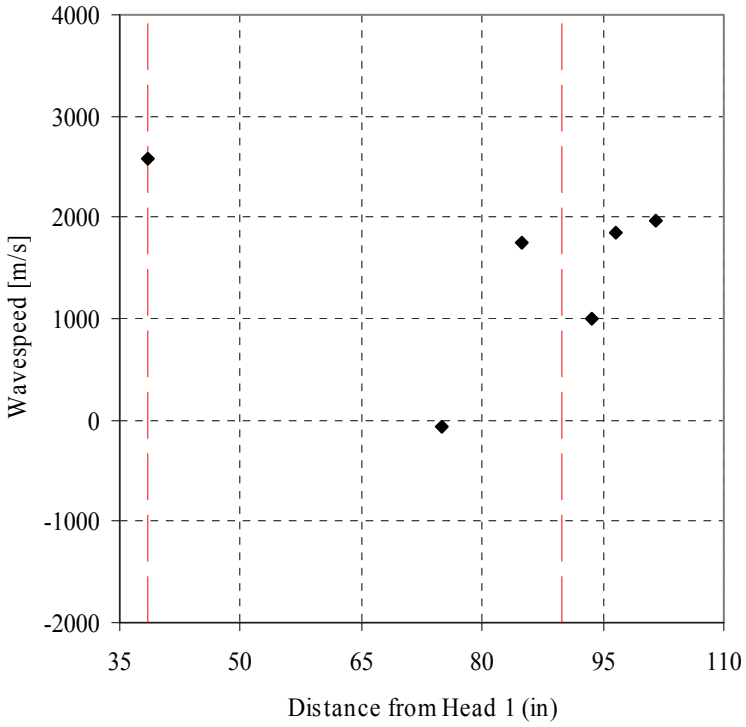

Figure 34. The responsible accompanying wave speeds for the pressure trace produced by a successful direct initiation shown in Figure 33

The magnitude of the plateau pressure displayed in Figure 33 is well below that of a typical detonation wave. This discrepancy is believed to be a calibration shift due to probe heating (Cooper et al., 2002). This effect was partially alleviated through the application of a layer of silicon-based sealant applied in an effort to protect the pressure transducers from the harsh environment of the PDE. It is believed however, that the relative pressures indicated by the pressure traces are accurate representations of the pressure trends in the head of the secondary detonation tube but are not absolute. Although quantitatively inaccurate, the transducers are believed to produce an accurate quantitative indication of the pressure in the head during the arrival of the successfully transferred detonation.

The head pressure trace of Figure 33 exhibits most characteristics of a direct detonation initiation: a brief spike in pressure, an elevated pressure plateau while the detonation wave travels the length of the tube and reflects back as an expansion wave and a blow down. There are a number of distinctive yet important differences that must be noted. First is the slight decrease in the plateau pressure at $t/t_{CJ} \sim 3$. This decrease is proposed to be due to a partial blow down through the crossover tube, resulting from the expansion that follows a typical detonation wave through the crossover tube at approximately half of the CJ wave speed. The second feature of notable interest is the pressure spike immediately prior to complete blow down. This is believed to be a result of the restrictor present on the tail-end of the secondary detonation tube. As the detonation wave reaches the end of the tube, it encounters a decrease in diameter and it is proposed that the wave is reflected back partially as a compression wave from the solid surface of the reducer and also as an expansion from the interface with the atmospheric air at the opening of the tube. Arriving back at the closed end of the secondary tube, the alleged compression wave followed closely by the expansion wave is seen through the pressure transducer as a brief pressure rise followed by blow down.

Unsuccessful Detonation Transfer

In order to better verify the successful direct initiation, the head pressure trace of a transferred combustion event deemed unsuccessful by wave speeds was analyzed. Again the pressure is shown as a function of the non-dimensional time; the result is Figure 35. This data was collected during Run 2 which was the configuration used to initially study the secondary detonation tube.

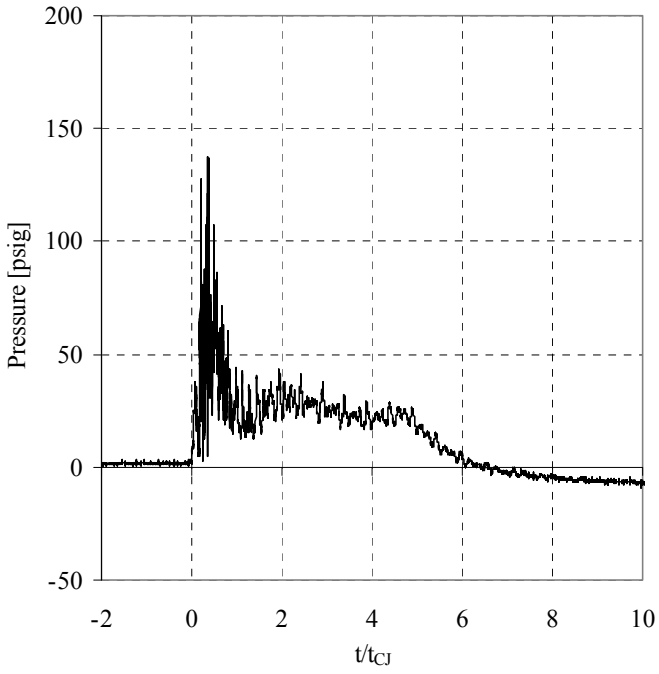

Figure 35. Secondary detonation tube head pressure trace as a function of non-dimensional time for an unsuccessful direct initiation

It becomes evident by examining the accompanying wave speed measurements shown in Figure 36 that the combustion event does not continue down the secondary tube as a detonation. The final measured wave speed for this trace is well below the steady-state Chapman-Jouguet detonation wave speed at 672 m/s.

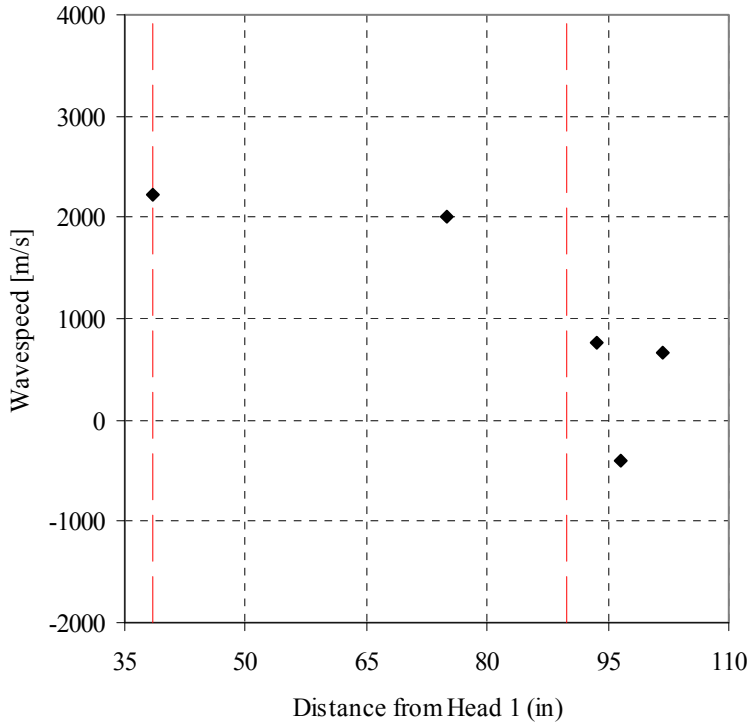

Figure 36. The responsible accompanying wave speeds for the pressure trace produced by an unsuccessful detonation transfer shown in Figure 35

The immediate decrease in pressure from the arrival of the transferred shock wave is not recovered downstream as would be the case if a detonation were to exist. This solidifies the wave speed measurement indication that a detonation is not present. Also, the extended overall duration when compared to the successful case shown above indicates that the combustion event was traveling at a much slower speed. It is believed that this slower moving combustion front is responsible for sustaining the slightly elevated pressure until it exits the detonation tube and equilibrium is achieved through blow down.

Reinitiation Event

Figure 37 is a pressure trace similar to those shown previously only in this case, the detonation wave appears to initially decouple upon emergence from the crossover tube.

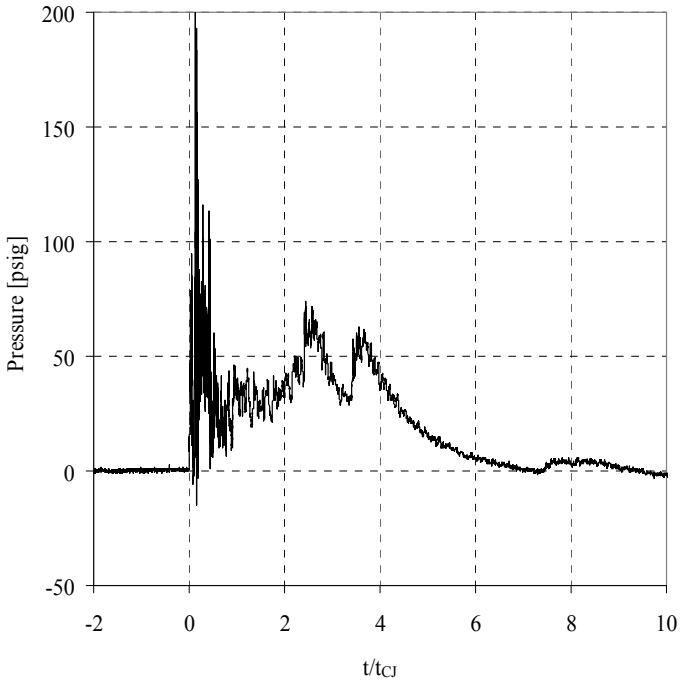

Figure 37. Secondary detonation tube head pressure trace as a function of non-dimensional time for a perceived reinitiation event

This decoupling is indicated by the low wave speeds measured at the 93.5 inch and 96.5 inch locations shown in Figure 38; the final wave speed however lends to the belief that the detonation then reinitiates downstream.

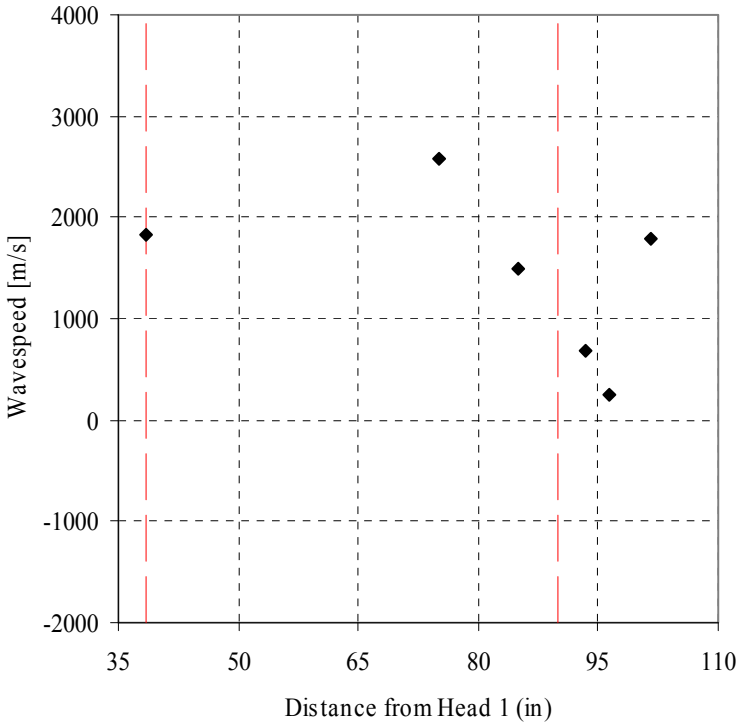

Figure 38. The responsible accompanying wave speeds for the pressure trace produced by a perceived reinitiation event shown in Figure 37

This data was collected using the setup parameters for Run 4 as set forth in Table 3 and was the only run conducted at an equivalence ratio of 0.9. All other variables, engine parameters and physical geometries were maintained the same as for those during Run 3. The pressure plateau recorded is at a lower value than the direct initiation case discussed previously and exhibits considerable variation. At the non-dimensionalized time value of approximately 2.5, the pressure rapidly increases likely indicating a retonation wave from the re-initiation event. This is followed by a pressure decrease believably corresponding to an expansion caused by the presence of the crossover tube, as discussed in reference to Figure 33. The similarly alleged compression and expansion waves traveling back towards the head are believed to result in a similar increase in pressure just prior to blow down. The delay in arrival (when compared to that of a

successful detonation transfer pressure trace) is likely due to the additional time required for the re-initiation event. The wave speed traces that accompany the two pressure traces presented above may indicate the importance of the pickup detonation wave speed to the ultimate success of the detonation propagating into the secondary thrust tube. For the purpose of comparison with Figure 34, the pickup wave speed recorded in Figure 38 is below that of the CJ value at 1833 m/s.

Previous Detonation Transfer Comparison

This research is the first to consistently directly initiate a detonation through the employment of detonation branching. Previous related work has been conducted by numerous people including but not limited to Helfrich, Panzenhagen and Slack. The results produced by these researchers has provided the basis for the current research and has virtually eliminated hours of trial and error. Most effort to date has been placed on measuring the effect of detonation branching on the engine characteristics such as ignition and DDT time. The most recent branch detonation work was conducted by Slack using the liquid hydrocarbon fuel JP-8. He conducted a comparison of the head pressure data obtained through spark and detonation initiated combustion events (Slack, 2007:56). The data was collected using similar pressure transducers and the same data acquisition system used for the current research, resulting in pressure data very similar to those present above. The data obtained from the branched detonation setup Slack used was modified to match the formatting of the head pressure data presented thus far. The major changes included the calculation of the Chapman-Jouguet time (t_{CJ}) for the different tube configuration and displaying the pressure trace data in a format similar to those presented

previously here to facilitate ease of comparison. The result is Figure 39 which contains the pressure trace collected during a run fueled with JP-8 of the secondary detonation tube head pressure trace.

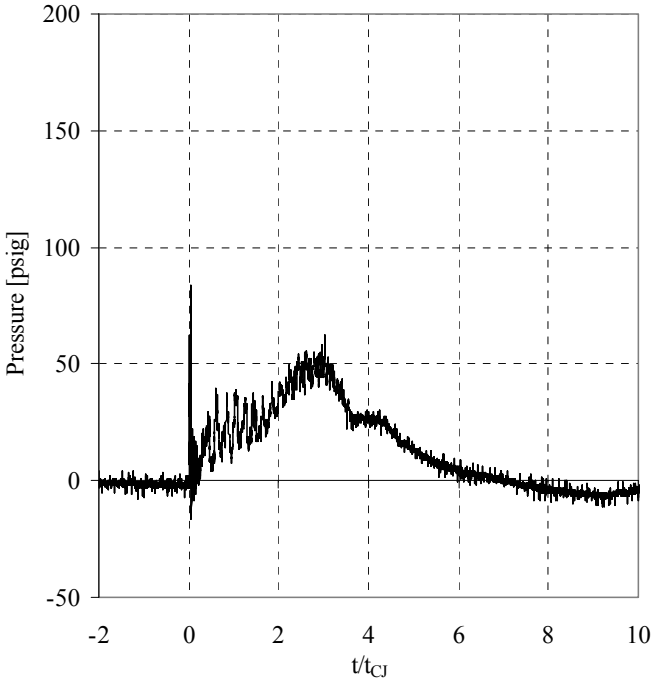

Figure 39. Pressure trace of previous branch detonation work using JP-8 shown as a function of non-dimensional time (Slack, 2007)

For similar reasons, the analysis of this pressure trace should be purely qualitative. The first observation that can be made is the difference between the amplitude of the pressure spike observed by the transducers upon arrival of the detonation wave. The peak of the initial pressure spike from the previous detonation branching data is less than half of that reported from the current research. The next observation is unveiled when focus is directed to the trend of the pressure development. The gradual pressure rise after the initial spike is more indicative of the head pressure trace associated with a typical spark ignited and hardware initiated detonation setup (not shown). This is to be expected here as the peak in pressure was obtained by the presence

of a hardware initiated detonation downstream. Had there been no DDT hardware in place and hence no detonation, the pressure trace would most likely have resembled the unsuccessful case above.

The sharp pressure rise is an indication of the entrance of the detonation wave. If the shock portion of the detonation wave survived the diffraction process there would be a step increase in the pressure trace, as is illustrated in Figure 33. There is no such step pressure increase in Figure 39 indicating that the shock wave failed upon expansion. This, coupled with the associated wave speed data from near the head of the secondary detonation tube (also not shown), further indicates the detonation wave did not successfully transition from the crossover during the previous research. From the previous detonation branching research, it was noted that the head pressures associated with detonation branching and spark ignitions were seen to be nearly equivalent in terms of peak magnitude when using JP-8, excluding the initial pressure spike of the branched case (Slack, 2007: 57). There is no such comparison for the current research; however the plateau magnitude is sustained at a higher level as is revealed between a comparison of Figure 33 and Figure 39.

V. Conclusions and Recommendations

Conclusions

This research was the first to date to present the successful and repeatable direct initiation of a detonation in a secondary detonation tube through the employment of detonation branching. The initial focus of this effort was ensuring successful detonation branching and sustaining the detonation throughout the entire crossover tube. This was necessary to ensure that strong detonations were presented to the junction of the crossover and the secondary tube where the detonation failure was most likely. Minor changes were made to the test setup (i.e. the 25% reduction in tail-end diameter) and the goal of obtaining CJ or greater wave speeds in the secondary thrust tube was accomplished. These wave speeds indicate a successful direct detonation initiation in the secondary tube and were obtained without the employment of internal DDT hardware (i.e. Schelkin-like spirals). This accomplishment is believed to be due in part to the transition device designed specifically for this research which causes a redirection of the detonation just prior to entering the secondary detonation tube.

Qualitative pressure traces were also presented, one which is indicative of a detonation striking the closed end of the secondary detonation tube. A qualitative analysis of the pressure traces reveals a characteristic direct detonation initiation in some cases and a decoupling/re-initiation in others; both exhibit some hardware-specific artifacts. A comparison with pervious branch detonation work was conducted, further solidifying results obtained through the qualitative analysis.

Recommendations for Future Work

There are numerous research topics that can be examined to determine the conditions necessary to continue the field of direct initiation by detonation branching. In order to better understand the method in which the crossover tube is filled and purged, it is suggested that a detailed pressure analysis be conducted. Examining the pressures at either end of the crossover tube as a function of time could give much needed insight as to the direction from which the crossover tube is filled. With the wave speed data presented here, the detonation wave travel could be superimposed on the fill information collected and possible areas of weak reactants or poor mixture quality where the detonation may be reduced in strength and/or fail completely could be realized and possibly eliminated.

Armed with the knowledge of how the detonation branching setup reacts over the course of the fill-fire-purge cycle, a subsequent step to the eventual implementation of detonation branching technology is to focus on success with more commercially accepted fuels (i.e. AV Gas, JP-8, etc.). Testing the setup with Hydrogen at reduced equivalence ratios will increase the cell size to the order of higher chain length hydro-carbon fuels and would be a logical first step.

Coupled with the alternate fuel work, the internal geometry at the point of union between the crossover and the secondary thrust tube may also be a focal point of future research. The concept of shock reflections has been seen to be advantageous in the formation of a detonation (de Witt et al., 2005) and as such could be employed at this connection to aid in either maintaining the coupling of the shock and combustion front or by reinitiating a new detonation altogether.

Appendix A: Data Reduction and Error Analysis

Data Reduction

PT Finder

The C++ program created to perform data reduction, *PT Finder*, begins by converting the acquired binary data into floating point values using the curve fit accompanying the file. The program then segments the data into separate cycles as denoted by the spark signals. Every spark incident indicates the beginning of a new firing cycle. A number of behind-the-scenes operations take place including, but not limited to, a smoothing filter, linear regression calculations, determining of ignition time and determining of DDT time and location. The result is a series of output files containing time stamps and signal magnitudes that can be displayed for the individual combustion events in a fashion similar to that shown in Figure 40.

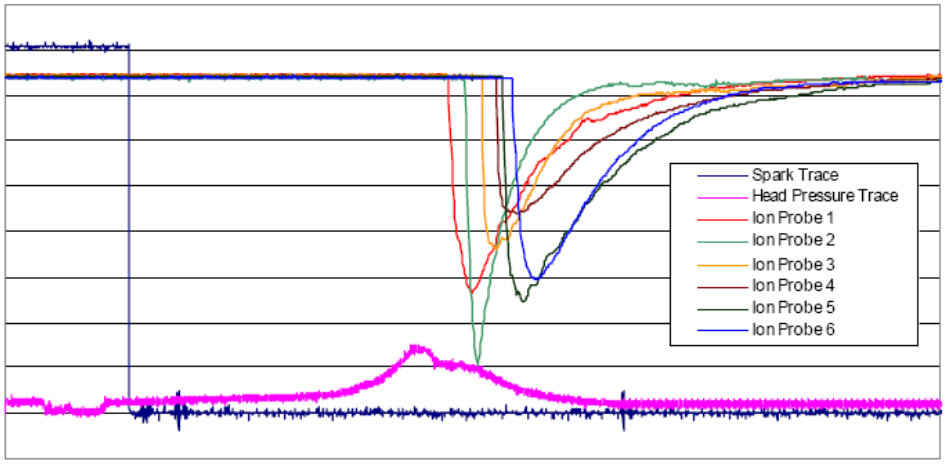

Figure 40. Example output traces of an individual combustion event from *PTFinder*

Wave Speed Calculations

The program then determines the time stamp of the various ion probe discharges as required by the user. As mentioned, the voltage discharge occurs at the time the

combustion wave passes the probe due to the completion of the circuit with the ions present. The program averages the first 1000 points in order to determine the baseline value of the individual ion probe signal and then searches for the first 500 point consecutive drop in voltage. The probe time is the first of the 500 points and in conjunction with the distances between ion probes, the wave speeds are calculated and sent to a spreadsheet. The sharp drops in voltage as indicated by ion probe traces shown in Figure 40 are qualitatively indicative of the passing of a detonation.

Error Analysis

The total uncertainty of a system is determined through a combination of bias and precision error. Bias error is a measurement of error that remains constant in magnitude for all observations; a type of systematic error. It is also present throughout the process of data reduction. Precision error is more a level of the variation of measurements and calculations. The total uncertainty is determined through a combination of the two:

$$U_{\bar{r}} = \sqrt{B_{\bar{r}}^2 + P_{\bar{r}}^2} \tag{21}$$

where $U_{\bar{r}}$ is the *total uncertainty*, $B_{\bar{r}}$ is the *bias*, $P_{\bar{r}}$ is *the precision error*, and r is the experimental result of interest (Coleman, 1989:7,94-95).

Precision Error

The precision error varies for each data point. Many average wave speed values are reported in the results section of this research. This average is determined using an equation to determine the experimental mean:

$$\bar{x} = \frac{\sum_{i=1}^{n} x_i}{n} \tag{22}$$

where $\bar{x}$ is the *average* of the data, x_i is an *individual data point*, and n is the *number of data points in the set* (Milton, 2003:203). The average for a given set of information represents the approximate trend of that data. However, while performing this method there is no measure of precision. To determine the precision of the experimental mean, the standard deviation is calculated:

$$\sigma = \sqrt{\frac{\sum_{i=1}^{n} (\bar{x} - x_i)^2}{n-1}} \tag{23}$$

where σ is the *standard deviation* (Milton, 2003:207).

Bias Error

Various parameters are often measured directly and have an inherent bias error due in part to their individual measurement devices. These are determined by using the root-sum-square equation shown below:

$$B_{\bar{r}} = \sqrt{\sum_{i=1}^{n} B_i^2} \tag{25}$$

Often times an experimental factor is a function of numerous different measurements that each carries their own bias. These individual effects of these elemental bias uncertainties are combined to determine the desired result using a modified form of the root-sum-square:

$$B_{\bar{r}} = \sqrt{\sum_{i=1}^{n} \left[\left(\frac{\partial r}{\partial X_i} \right)^2 B_i^2 \right]} \tag{26}$$

Where B_r is the *bias of the variable of interest*, r is the *variable of interest*, and B_i is the *bias of each measured variable* (Coleman, 1989:79). Bias errors were calculated for a variety of the parameters discussed previously.

Pressure Transducer Uncertainty

The pressure transducers used in this research measure a voltage which is converted to a pressure reading. The transducers are calibrated to within 0.1% of the measured voltage. If the maximum voltage is 0.05 V for example, the resulting transducer calibration uncertainty would be ±0.05 mV. The response time associated with these pressure transducers is known to be within 1 μsec, thereby resulting in ±0.5 μsec rise time uncertainty (Helfrich, 2006:73). These uncertainties most directly affect the ignition time calculation of the primary detonation tube which is not addressed in the current research.

Air Mass Flow Rate Uncertainty

The air mass flow rate is a function of the pressure transducer, thermocouples, and critical flow nozzles as described above. The pressure transducers are accurate to 0.1% of the full scale value and which is ±413.68 Pa. The error of the T-Type thermocouple used is ±3 K. The radius of the critical flow nozzles are accurate to within ±0.0005 in. The resulting uncertainty of the air mass flow rate is ±0.127 lb_m/min.

Wave Speed Uncertainty

The wave speed is a function of the distance between the ion probes and their response time. The ion probes response time of 0.1 μsec results in an uncertainty of ±0.5

μsec. In addition, the ion probe locations were measured to within 1/16 inch which is an uncertainty of ±1/32 inch. This results in an uncertainty of approximately ±7.53 m/s. As mentioned previously, the calculated wave speed is assumed and, therefore, reported to be located at the midpoint of the two ion probes used. In actuality, the wave speed is merely an average of the wave speed as it travels between the two probes and could occur anywhere between the two locations. This uncertainty will transmit through to DDT time and location calculations. As neither of these values are analyzed and reported in the current research, the further uncertainty analyses are not conducted.

Bibliography

Coleman, Hugh W. and Steele, W. Glenn, Jr. *Experimentation and Uncertainty Analysis for Engineers*. New York NY: John Wiley and Sons Incorporated, 1989.

Cooper, M., Jackson, S., Austin, J., Wintenberger, E. and Shepherd J.E., "Direct Experimental Impulse Measurements for Detonations and Deflagrations," *Journal of Propulsion and Power*, Vol. 18, No. 5, Pg. 1033-1041, Sep-Oct 2002.

de Witt, B., Ciccarelli, G., Zhang, F., Murray, S., "Shock Reflection Detonation Initiation Studies for Pulse Detonation Engines," *Journal of Propulsion and Power*, Vol. 21, No. 6, Pg. 1117-1125, Nov-Dec 2005.

Eidelman, S., Grossman, W., and Lottati I. "Review of Propulsion Applications and Numerical Simulations of the Pulse Detonation Engine Concept," *Journal of Propulsion and Power*, Vol. 7:6, (November – December 1991).

Fickett, Wildon and Davis, William C. *Detonation: Theory and Experiment.* New York NY: Dover Publications Incorporated, 1979.

Glassman, Irvin. *Combustion (3rd Edition)*. Sand Diego CA: Academic Press, 1996.

Helfrich, Timothy M. *Cycle Performance of a Pulse Detonation Engine with Supercritical Fuel Injection*. Air Force Institute of Technology (AU), Wright-Patterson AFB OH. March 2006.

Kuo, Kenneth K. *Principles of Combustion (2nd Edition)*. Hoboken NJ: John Wiley and Sons Incorporated, 2005.

Kaneshige, M. and Shepherd, J.E. *Detonation database***.** Technical Report FM97-8, GALCIT, July 1997. See also the electronic hypertext version at http://www.galcit.caltech.edu/detn_db/html/.

Milton, J. Susan and Arnold, Jesse C. *Introduction to Probability and Statistics: Principles and Applications for Engineering and the Computing Sciences*. New York NY: McGraw-Hill Higer Education, 2003.

Miser, Christian L. *Pulse Detonation Engine Thrust Tube Heat Exchanger for Flash Vaporization and Supercritical Heating of JP-8*. MS Thesis, AFIT/GAE/ENY/05-M11. Graduate School of Engineering and Management, Air Force Institute of Technology (AU), Wright-Patterson AFB OH. March 2005.

Oran, E.S., Young, T.R., Boris, J.P., et al., "A Study of Detonation Structure: The Formation of Unreacted Gas Pockets," NRL Memorandum Report 4866, 26 July 1982, Naval Research Laboratory, Washington, DC 20375.

Panzenhagen, Kristin L. *Detonation Branching in a PDE with Liquid Hydrocarbon Fuel*. MS thesis, AFIT/GAE/ENY/04-M14. Graduate School of Engineering and Management, Air Force Institute of Technology (AU), Wright-Patterson AFB OH. March 2004.

PCB Piezotronics. "Introduction to Piezoelectric Pressure Sensors." http://www.pcb.com/techsupport/tech_pres.php.

Rolling, August J. *Alternative Pulse Detonation Engine Ignition System Investigation Through Detonation Splitting*. MS thesis, AFIT/GAE/ENY/02-10, Graduate School of Engineering and Management, Air Force Institute of Technology (AU), Wright-Patterson AFB OH. March 2002.

Schultz, Eric. *Detonation Diffraction Through an Abrupt Area Expansion*. Dissertation. California Institute of Technology, Pasadena CA. April 2000.

Schauer, Frederick R, Stutrud, Jeffery, and Bradley Royce P. "Detonation Initiation Studies and Performance Results for Pulse Detonation Engine Applications," 39th AIAA Aerospace Sciences Meeting and Exhibit. Reno NV: AIAA 2001-1129, 8 – 11 January 2001.

Slack, David J. *Branched Detonation of a Pulse Detonation Engine with Flash Vaporized JP-8*. MS thesis, AFIT/GAE/ENY/07-D04. Graduate School of Engineering and Management, Air Force Institute of Technology (AU), Wright-Patterson AFB OH. December 2007.

Tucker, K. Colin. *A Flash Vaporization System for Detonation of Hydrocarbon Fuels in a Pulse Detonation Engine*. Dissertation, AFIT/DS/ENY/05-03. Graduate School of Engineering and Management, Air Force Institute of Technology (AU), Wright-Patterson AFB OH. June 2005.

Tucker, K. Colin, King, Paul I., Schauer, Frederick R., and Hoke, John L. "Branched Detonation in a Multi-Tube PDE," *16th International Symposium on Air Breathing Engines*. Cleveland OH: ISABE 2003-1218, September 2003.

Vita

Second Lieutenant Alexander Robert Hausman graduated Gibsonburg High School of Gibsonburg, OH in May of 2001. He then attended The University of Toledo in Toledo, OH where he graduated Magna Cum Laude with a Bachelor of Science in Mechanical Engineering and a minor in Business Administration on 6 May 2006. He was commissioned as a Distinguished Graduate through Air Force ROTC Detachment 620 located at Bowling Green State University in Bowling Green, OH on 5 May 2006.

Lieutenant Hausman's active duty career began with a direct accession to the Air Force Institute of Technology, Graduate School of Engineering and Management for his Masters of Science in Aeronautical Engineering. The focus of his studies were in air breathing propulsion and aeroelasticity. Upon graduation on 27 March 2008, he will be assigned to the 651st Test Systems Squadron located at Arnold AFB, TN fulfilling the role of a project manager.

REPORT DOCUMENTATION PAGE

Form Approved
OMB No. 0704–0188

1. REPORT DATE (DD–MM–YYYY)	2. REPORT TYPE	3. DATES COVERED *(From — To)*
27-03-2008	Master's Thesis	September 2007 – March 2008

4. TITLE AND SUBTITLE

DIRECT INITIATION THROUGH DETONATION BRANCHING IN A PULSED DETONATION ENGINE

5a. CONTRACT NUMBER

5b. GRANT NUMBER

5c. PROGRAM ELEMENT NUMBER

6. AUTHOR(S)

Alexander R. Hausman, Second Lieutenant, USAF

5d. PROJECT NUMBER

5e. TASK NUMBER

5f. WORK UNIT NUMBER

7. PERFORMING ORGANIZATION NAME(S) AND ADDRESS(ES)

Air Force Institute of Technology
Graduate School of Engineering and Management (AFIT/EN)
2950 Hobson Way
WPAFB OH 45433-7765

8. PERFORMING ORGANIZATION REPORT NUMBER

AFIT/GAE/ENY/08-M17

9. SPONSORING / MONITORING AGENCY NAME(S) AND ADDRESS(ES)

AFRL/RZTC
Attn: Dr. Fred Schauer
1790 Loop Road
WPAFB OH 45433-7765

10. SPONSOR/MONITOR'S ACRONYM(S)

11. SPONSOR/MONITOR'S REPORT NUMBER(S)

12. DISTRIBUTION / AVAILABILITY STATEMENT

APPROVED FOR PUBLIC RELEASE; DISTRIBUTION UNLIMITED.

13. SUPPLEMENTARY NOTES

14. ABSTRACT

Pulsed Detonation Engines are currently limited in operating frequency to the order of 40 Hz due to lengthy ignition and deflagration to detonation transition (DDT) times. An experimental study is conducted to determine the requirements necessary to eliminate these constraints through the concept of direct initiation. A branched detonation crossover setup is constructed and the operational requirements are determined.

This research demonstrates the ability to directly initiate a detonation in a vacant tube from a detonation obtained through detonation branching. Using a hydrogen-air mixture, a tail-to-head detonation branching is achieved in which a detonation is seen to propagate from a spark ignited detonation tube, through a crossover tube and across a 1:2 diameter expansion ratio into a vacant second detonation tube. This effectively eliminates the ignition and DDT times associated with the conventional operation of the second tube. The closed-end pressure trace of a transferred detonation as deemed successful through wave speed measurements is analyzed and further solidifies the findings.

15. SUBJECT TERMS

Pulsed Detonation Engine, PDE, Detonation, Detonation Branching, Direct Initiation

16. SECURITY CLASSIFICATION OF:			17. LIMITATION OF ABSTRACT	18. NUMBER OF PAGES	19a. NAME OF RESPONSIBLE PERSON
a. REPORT	b. ABSTRACT	c. THIS PAGE			Dr. Paul I. King
U	U	U	UU	93	19b. TELEPHONE NUMBER (Include Area Code) (937) 255-6565, ext 4628; e-mail: paul.king@afit.edu